

World Maritime University

The Maritime Commons: Digital Repository of the World Maritime University

Maritime Safety & Environment Management
Dissertations (Dalian)

Maritime Safety & Environment Management
(Dalian)

8-27-2021

Study on emergency response mechanism and treatment technology of LNG releasing on/under water

Bin Zhang

Follow this and additional works at: https://commons.wmu.se/msem_dissertations



Part of the [Emergency and Disaster Management Commons](#), and the [Oil, Gas, and Energy Commons](#)

This Dissertation is brought to you courtesy of Maritime Commons. Open Access items may be downloaded for non-commercial, fair use academic purposes. No items may be hosted on another server or web site without express written permission from the World Maritime University. For more information, please contact library@wmu.se.

WORLD MARITIME UNIVERSITY

Dalian, China

**STUDY ON EMERGENCY RESPONSE
MECHANISM AND TREATMENT TECHNOLOGY
OF LNG RELEASING ON / UNDER WATER**

By

Bin Zhang

The People's Republic of China

A dissertation submitted to the World Maritime University in partial
Fulfillment of the requirements for the award of the degree of

MASTER OF SCIENCE

In

(MARITIME SAFETY AND ENVIRONMENTAL MANAGEMENT)

2021

© Copyright , 2021

Declaration

I certify that all the material in this dissertation that are not my own work have been identified, and that no material is included for which a degree has previously been conferred on me.

The contents of this dissertation reflect my own personal views, and are not necessarily endorsed by the University.

Signature: *Bin Zhang*

Date: 2021.8.30

Dalian Maritime University

Assessor:

Co-assessor:

Acknowledgement

Firstly, I would like to thank World Maritime University and Dalian Maritime University for giving me the opportunity to further explore the maritime field, and thank all my professors who lecture on the various subjects during the entire MSEM course.

Secondly, I would like to thank my supervisor, Professor Wu Wanqing. Throughout the process of writing this paper, he always gave me unremitting support and patient help with his profound professional knowledge, rigorous academic attitude, and approachable personality. A lot of efforts were put into supervising this paper. Therefore, I would like to express my deep gratitude and sincere blessings to him.

Thirdly, my family always give me meticulous care and unlimited support in the process of the whole studying process, so that I can finally complete this work without fear of various challenges. I would express my sincere thanks to my family.

Finally, this work is supported by National Natural Science Foundation of China (51306026), Liaoning Provincial Natural Science Foundation of China (201602087) the Fundamental Research Funds for the Central Universities (3132016015) and (3132016350), Fundamental Research Funds for Maritime Safety Administration of China (2013-60).

Abstract

Title of Dissertation: Study on emergency response mechanism and treatment technology of LNG releasing on/under water

Degree: MSc

The rapid development of the LNG shipping industry has led to a significant increase in the number of ships, ship tonnage, and ship speed. However, as the density of routes increases, coupled with the influence of weather and human factors, the probability of LNG ship leakage accidents have increased. In order to ensure the safety of LNG maritime transportation and personnel safety, this paper makes a study on emergency response mechanism and treatment of LNG releasing on/under water.

Firstly, an experimental system is designed and fabricated to visually investigate explosive boiling mechanism of cryogen injection into water. Visualized results show that LNG and LN₂ injection processes undergo a similar boiling, that is explosive boiling, which is characterized by bubbles cloud that strengthens heat transfer rate. The maximum heat transferring flux can be over 1.9 MW/m² in the condition of LNG injection into unconfined water and under the pressure of 7 bars. In order to investigate the determinant factors for explosive boiling occurring, instability of Rayleigh-Taylor, Kelvin-Helmholtz, Weber number and Marangoni convection are analyzed and used to explain the differences of maximum pressure and its occurring time in different experimental conditions such as injection depth into water, injection pressure, water temperature and injecting fluid.

Secondly, a numerical model is built up to simulate the whole releasing process. Based on the results, in the case of explosion boiling, with the spreading of the LNG pool on the surface, several times explosion boiling occurs intermittently, with the first one being the most intense. It can be considered that in the process of accident treatment, not only to prevent low temperature frostbite, flammable gas diffusion, but also to prevent the occurrence of uninterrupted explosion boiling. The occurrence of explosion boiling has no effect on the maximum liquid pool expansion radius, because the maximum liquid pool expansion radius occurs before it. However, it has a great influence on the duration time of liquid pool and the dispersion range of NG. The duration time of the LNG pool will shorten by nearly 10% with the occurrence of explosion boiling, and the diffusion range of combustible gas will expand by 5%.

Thirdly, an emergency response mechanism is established for LNG carrier leakage accidents and treatment methods for preventing explosive boiling occurring are proposed. The effectiveness of these treatment methods are analyzed by numerical simulation.

This research can not only limit the impact range, hazard level and disaster loss of LNG water leakage disaster to the greatest extent, but also has extremely important economic and practical significance for ensuring the rapid and stable development of the national economy. At the same time, it is also a breakthrough in the existing boiling theory and a supplement to the boiling research system, which has far-reaching academic significance.

KEY WORDS: LNG carrier; Explosive boiling; Emergency treatments; Releasing on/under water; NG dispersion; LNG pool spreading

Table of contents

Declaration	I
Acknowledgement.....	II
Abstract	III
Table of contents.....	V
List of Tables	VII
List of Figures.....	VIII
List of Abbreviations	IX
Chapter 1 Introduction.....	1
1.1 Background.....	1
1.2 Purpose and significance of the study	3
1.3 Research status	5
1.3.1 Experimental research status	5
1.3.2 Theoretical research status.....	7
1.3.3 Safety management status.....	9
1.4 Main contents of the study.....	12
1.5 Research methods and the technical route.....	13
1.5.1 Research methods	13
1.5.2 Technical route.....	17
Chapter 2 Experimental research.....	19
2.1 Experimental apparatus	19
2.2 Experimental results	21
2.3 Analysis of the experimental results	22
2.3.1 Heat transferring flux.....	22
2.3.2 Theoretical analysis about instability	23
2.3.3 Effect of injection depth into water	27
2.3.4 Effect of injection pressure.....	28
2.3.5 Effect of water temperature	29
2.3.6 Effect of injecting cryogen	31
2.3.7 Bubble behaviors analysis	33

Chapter 3 Numerical research	38
3.1 Numerical models.....	38
3.2 Numerical results of releasing on water	42
3.3 Numerical results of releasing under water	46
Chapter 4 Emergency treatments.....	50
4.1 Initial conditions	52
4.2 Results analysis	52
4.3 The emergency response on LNG releasing on water	54
4.4 The emergency response on LNG releasing under water	57
Chapter 5 Conclusion and Suggestions	59
5.1 Conclusion.....	59
5.1.1 Experimental research summary.....	59
5.1.2 Numerical research summary	60
5.1.3 Emergency treatments summary.....	61
5.2 Suggestions.....	61
References	63

List of Tables

Table 1-1	Proportion of energy consumption of major countries and the world in 2017....	1
Table 2-1	Experiment run parameters	21
Table 3-1	Substances Parameters for Tleidenfrost, TC, and TSLT.....	41
Table 3-2	Calculation results of releasing on water	42
Table 3-3	Calculation results of releasing under water	46
Table 4-1	Results of emergency treating on releasing on the water surface	53
Table 4-2	Results of emergency treating on releasing underwater 5m.....	54

List of Figures

Figure 1-1 Schematic diagram of LNG water area discharge experiment system.....	15
Figure 1-2 Technical roadmap of the research.....	18
Figure 2-1 Experimental system and apparatus: (a) picture of apparatus; (b) positions of all sensors in tank.	19
Figure 2-2 Pressure curve correspondent to run 1 using the P sensor under water: (a) the time is from 0 ms to 10000 ms after injection; (b) the time is from 5400 ms to 5499 ms after injection).....	23
Figure 2-3 Schematic diagram of Marangoni convection near the vapor film (The original image is 3d in Figure 2-5).....	27
Figure 2-4 Most dangerous wavelength in Rayleigh-Taylor instability and Kelvin-Helmholtz instability, and minimum characteristic length in Weber Number Theory	30
Figure 2-5 Bubble behaviors of cryogen injection into water (1a~1f are images of run 1, 2a~2f are images of run 6, 3a~3f are images of run 5. The interval time between the adjacent two images is 50 ms).	37
Figure 3-1 Releasing on water 0 m without Explosive Boiling (a. Releasing rate; b. Liquid Pool Mass; c. Liquid Pool Radius; d. Dense Gas Radius).....	44
Figure 3-2 Releasing on water 3 m without Explosive Boiling (a. Releasing rate; b. Liquid Pool Mass; c. Liquid Pool Radius; d. Dense Gas Radius).....	44
Figure 3-3 Releasing on water 3 m with Explosive Boiling (a. Releasing rate; b. Liquid Pool Mass; c. Liquid Pool Radius; d. Dense Gas Radius)	44
Figure 3-4 Releasing underwater 3 m without Explosive Boiling (a. Releasing rate; b. Liquid Pool Mass; c. Liquid Pool Radius; d. Dense Gas Radius).....	47
Figure 3-5 Releasing underwater 3 m with Explosive Boiling (a. Releasing rate; b. Liquid Pool Mass; c. Liquid Pool Radius; d. Dense Gas Radius).....	48
Figure 3-6 Releasing underwater 5 m with Explosive Boiling (a. Releasing rate; b. Liquid Pool Mass; c. Liquid Pool Radius; d. Dense Gas Radius).....	48
Figure 4-1 Floating plant design.....	55

List of Abbreviations

LNG	Liquefied Natural Gas
NG	Natural Gas
LC ₃ H ₈	Liquefied Propane
LN ₂	Liquefied Nitrogen
OPRC-HNS	International Protocol on Preparation, Response and Cooperation of Toxic and Hazardous Substances
SOLAS	International Convention for Safety of Life at Sea
ISPS	International Ship and Port Facility Security Code
STCW	International Convention on Standards of Training, Certification and Watchkeeping for Seafarers
IGC	International Code for the Construction and Equipment of Ships Carrying Liquefied Gases in Bulk
ICS	International Chamber Shipping
OCIMF	Oil Companies International Marine Forum
BV	Bureau Veritas
DNV	Det Norske Veritas
ABS	American Bureau of Shipping

Chapter 1 Introduction

1.1 Background

As the world's energy industry accelerates toward diversified, clean, and low-carbon development, the global demand for clean energy is growing rapidly. Natural gas is a clean energy source. The greenhouse gases produced after combustion are only 50% of coal combustion and 65% of oil combustion. The combustion products contain almost no sulfur, dust and other harmful substances, and the calorific value generated by combustion is higher than other fossil fuels. In my country's energy consumption structure, the ratio of natural gas is 7.1%, which is much lower than the world average, as shown in Table 1-1. According to the "13th Five-Year Plan for Energy Development", non-fossil energy and natural gas consumption will account for more than 68% of energy consumption by 2020, and natural gas energy will account for 10% of primary energy consumption.

Table 1-1 Proportion of energy consumption of major countries and the world in 2017

Country	Coal	Oil	Natural gas	Other
China	60.4%	18.8%	7.1%	13.7%
United States	14.9%	40.9%	28.4%	15.8%
Japan	26.4%	41.3%	22.1%	10.3%
United Kingdom	4.7%	39.9%	35.4%	20.0%
World	27.6%	34.2%	23.4%	14.8%

Since China has begun to import natural gas in 2006, the amount of natural gas imports has increased year by year, and the degree of dependence on natural gas resources has increased year by year. In 2018, China imported 125.4 billion m³ of natural gas,

surpassing Japan, becoming the world's largest natural gas importer. Import volume increased by 31.7%, and its external dependence increased to 45.3% (DIAO,2019). The increase in demand for natural gas has stimulated the development of the LNG (liquefied natural gas) shipping market. The increase in demand for natural gas has stimulated the development of the LNG shipping market. As for the first three quarters of 2018, 46 LNG ships were traded globally, more than three times the turnover of the whole year of 2017 (CAO,2018).

The rapid development of the shipping industry has led to a significant increase in the number of ships, ship tonnage, and ship speed. However, as the density of routes increases, coupled with the influence of weather and human factors, the probability of ship accidents have increased. From 2011 to 2015, 99 ship collision accidents occurred in Zhoushan waters, accounting for about 62% of the total number of accidents (WU,2017); From 2002 to 2015, 42 ship collision accidents occurred in the jurisdiction of Qingdao Maritime Safety Administration, accounting for 42.4% of the total number of accidents(ZHANG,2017); Maritime statistics from the Hong Kong Maritime Department show that there were 1,664 ship accidents of various types in Hong Kong waters during the five-year period from 2013 to 2017, of which 711 collisions, accounting for 42.73%.

LNG ship is the main tool of natural gas transportation by sea. It is a kind of high economic value-added ship, and it is also a dangerous cargo ship. According to relevant organizations such as DNV, Lloyds, SIGTTO, OSC, etc., there are 45 LNG ship accidents recorded in detail as of 2010, of which 10 occurred when the ship was loaded, accounting for about 22% of the total accidents. There were 8 cases, accounting for about 18% of the total number of accidents, 19 cases occurred during navigation, accounting for about 42% of the total number of accidents, and 18 cases

were recorded due to leakage, accounting for about 40% of the total number of accidents (KANG,2019).

LNG ships are known as "super-refrigerated vehicles at sea", and they transport liquefied natural gas (LNG) formed by cooling natural gas to an ultra-low temperature of minus 160°C. When the hull structure of an LNG ship is damaged due to a collision accident, it may cause the LNG in the cargo tank to leak. The entry of volatile and flammable LNG into the environment will cause huge losses to the hull, the safety of personnel, and the marine environment. The LNG leaked at sea meets certain conditions. Due to the huge temperature difference, LNG absorbs heat from the environment, the evaporation rate of LNG increases rapidly, and an explosion occurs. This phenomenon is called rapid phase transition, and this phenomenon is also called rational phase transition. The leaked LNG absorbs heat to form a cloud of LNG vapor. The mixed gas of LNG vapor and air is within the explosion limit and explodes upon fire. Therefore, carrying out LNG water leakage research is of great significance to ensure the safety of LNG maritime transportation and personnel safety.

1.2 Purpose and significance of the study

Based on the current research status, social development, maritime safety and regulatory needs, this research adopts numerical research, theoretical analysis and experimental research, combining qualitative analysis and quantitative analysis, and researches on LNG water leakage emergency response mechanism and treatment technology. Build up a visual observation platform for LNG water discharging, use advanced high-speed dynamic recording methods and temperature and pressure measurement techniques to calibrate the important factors that affect the boiling mode

of LNG waters (in view of the greater danger of explosive boiling, focus on the observation of explosive boiling Mode), and give the boiling rate calculation model under each boiling mode, and propose a method to control the mutual transition of the boiling mode.

On the basis of the experimental results of dynamic mechanism, the CFD technology is used to carry out numerical simulation research on the flow and mass transfer process of LNG water leakage multiphase flow, and is connected with the NG gas atmospheric diffusion model, and a set of experimental data support is developed. A theoretically based calculation software for LNG water leakage and atmospheric dispersion.

Summarize the current LNG loading and unloading terminal and ship supervision and management status, emergency response mechanism and accident handling technology. Based on the experimental data and theoretical analysis of LNG water area discharge, researchers propose a more scientific and applicable LNG ship water area leakage emergency response mechanism, and develop control The boiling rate and the processing technology of changing the boiling mode make the leaked LNG liquid boil in a stable and gentle manner in the water area, so that the NG gas can be diluted to below the explosion range in a very short time, thereby reducing and limiting its hazards Scope and hazard level.

This research can not only limit the impact range, hazard level and disaster loss of LNG water leakage disaster to the greatest extent, but also has extremely important economic and practical significance for ensuring the rapid and stable development of the national economy. At the same time, it is also a breakthrough in the existing boiling theory and a supplement to the boiling research system, which has far-reaching

academic significance.

1.3 Research status

1.3.1 Experimental research status

When an LNG ship has a water leakage accident, it can be divided into leakage on water and leakage underwater according to the location of the hole in accident. At present, most of the experimental studies mainly study the low-temperature liquid pool range formed by the LNG leakage, the gas diffusion range and concentration field changes, and the explosion of LNG when the LNG leaks from the water surface and the land surface. On the other hand, there are very few leakage experiments under water LNG, and the representative experiments include:

Maplin Sands(D.R.BLACKMORE,1982;J.S.PUTTOCK,1982;R.P.KOOPMAN,1982) series of experiments, this series of experiments carried out underwater leakage experiments containing 10 groups of LNG or liquid propane. The study found that the diffusion of gas produced by boiling is related to the way of leakage. The vapor cloud caused by underwater leakage has a higher floating height and a short horizontal diffusion distance, while a water surface leakage produces a lower level of vapor cloud that diffuses over a longer distance. One group of experiments observed a rapid phase transition, and the maximum pressure generated was 1.8 kPa. Ruifeng Qi (QI,2011) and others conducted an underwater LNG release test and constructed a pit with a size of 10.06 m × a depth of 6.4 m, a depth of 1.22 m, and a water depth of 1.14 m. At 0.71 m below the surface of the water, a LNG jet hole that shoots vertically upwards is released through a pipe with a diameter of 25.4 mm. Use underwater cameras to record underwater phenomena, use land-based cameras to capture surface

and aerial phenomena, analyze LNG boiling phenomena, and determine the characteristics of the steam emitted from the water surface.

In addition, scholars have carried out some researches on the releasing underwater process of cryogenic liquids, which can provide certain guidance for LNG underwater leakage. Representative experiments include:

D.S.Wen (WEN,2006) conducted an experiment of releasing a small amount of liquid nitrogen into the water. By monitoring the pressure and temperature changes after the liquid nitrogen was sprayed into the water, the pressure change and heat exchange during the phase change process of the liquid nitrogen was analyzed. The heat flux of the boiling is like that of the boiling occurring in the rough tube. Clarke H(H.CLARK,2010) studied the liquid column structure of liquid nitrogen injection into water, using a high-speed camera to photograph the evolution process of liquid nitrogen injection into the water. The injection and decomposition can be divided into gaseous pre-injection phase, liquid injection, and collision with the column. They found that a thick vapor layer is formed around the liquid nitrogen core, and the rupture is mainly caused by the collision with flow instability. Duckworth(R.C.DUCKWORTH,2001) and Archakositt(ARCHAKOSITT,2004) et al. simulated the interaction between fuel and refrigerant by pouring a small portion of water into a liquid nitrogen pool. In these studies, they found that ice formation in the liquid nitrogen pool was like the quick frozen food process. Shu(ARCHAKOSITT,2019) et al conducted experiments on the release of liquid nitrogen under normal pressure and pressurized water, estimated the survival distance of the cryogenic liquid column, measured the temperature change of the water area, recorded the underwater boiling phenomenon of liquid nitrogen through video. They suggests that the heat transfer coefficient of liquid nitrogen can reach $20 \text{ kW}/(\text{m}\cdot\text{K})$

when boiling underwater. Guo (GUO,2005) conducted underwater atmospheric discharge of cryogenic liquid, analyzed the discharge flow pattern and ice layer growth, and simulated the growth process and shape of the ice layer. Zhang(ZHANG,2017) established a visual experimental system for the LN₂ releasing into water. The results show that the pressure difference significantly affects the ice formation speed and the survival distance of the liquid. Adding a nucleating agent helps provide ice cores and accelerate the ice formation speed. The water flow has a certain effect on changing the pressure difference, which will affect the freezing speed and the survival distance of the liquid. Gao (GAO,2014) studied the heat transfer process between LN₂ and water, built a visual observation platform for LN₂ discharging into water. He put forward the criteria for judging whether the explosive boiling occurs or not.

1.3.2 Theoretical research status

The underwater leakage process of LNG is quite complicated. Not only does it have a multiphase flow of mass and heat transfer, but it is also accompanied by a process of explosive boiling.

Porteous(PORTEOUS,1976) and Reid(REID,1983) proposed that only when the water temperature is between 1 to 1.5 times the LNG superheating limit temperature, the explosion boiling can occur. Nail(NAIL,1999) established a mathematical model for the rapid phase change of LNG droplets falling into the water to simulate the behavior of liquefied natural gas droplets. The model ignores the formation and growth of bubbles. From the perspective of energy and mass transfer, it analyzes LNG droplets and the environment. The phase change process of the water contact interface. Dmitrill(DMITILL,2003) corrected the surface tension coefficient of the bubbles in

the superheated liquid, and obtained the correlation length of density fluctuation and the evaporation coefficient through calculation. Park (PARK,2001) found that only from the micro-scale aspect of the thermodynamic theory, the microscopic process cannot be described fundamentally, but the observed bubble nucleation phenomenon can only be described from a qualitative perspective. Morshed (MORSHED,2011) simulated the explosive boiling phenomenon of liquid argon on the surface of nanostructured solids through molecular dynamics theory, and proposed that the problem of explosive boiling on part of the solid-liquid interface can be explained by molecular dynamics theory. Dong(DONG,2005) established a saturated liquid nitrogen explosion boiling tests to analyze the explosion boiling phenomenon of saturated liquid nitrogen under pulsed laser heating. According to the characteristics of the initial explosion boiling, he established an initial dynamic model of saturated liquid nitrogen based on the internal characteristics of the bubble group. The heat transfer mechanism model of the explosive boiling period is established. Liu(LIU,2016) established a mathematical model for analyzing the rapid phase change of LNG underwater, and performed a numerical simulation on the Clarke H experiments.

In the process of LNG leakage under water, due to hydraulic instability, pressure wave, water flow, gravity and other factors, LNG droplets will rupture and fragment, resulting in a sharp increase in heat exchange. In the study of hydraulic and thermal fragmentation, scholars have carried out some researchs.

Teng(TENG,2003) studied the interfacial instability of LCO₂ during deep-sea jetting. Based on the Rayleigh maximum instability theory, he established a rupture time model, and compared and analyzed the effect of CO₂ on the rupture time during the hydration process. Abe(ABE,2004) found that due to the Rayleigh-Taylor instability,

small disturbances on the gas-liquid interface grow rapidly, forming a coolant jet toward the surface of the molten droplet, which promotes the thermal fragmentation of the molten particles. Yuan(YUAN,2008) used the VOF interface tracking model to simulate the thermal fragmentation process of molten droplets under the action of pressure pulses, and found that droplet deformation and the hydraulic instability of the droplet surface are caused by droplet fragmentation.

1.3.3 Safety management status

At present, China has established a relatively complete oil pollution response system, including the establishment of a national oil pollution gradual response system, requirements for ships to formulate oil pollution emergency plans, shipping companies to formulate corresponding oil pollution response systems, and port units forming a joint defense body, etc., to effectively control The damage caused by pollution accidents in Chinese waters has been achieved, and the expected results have been achieved. However, with the entry into force of the OPRC-HNS Protocol (International Protocol on Preparation, Response and Cooperation of Toxic and Hazardous Substances), how to establish an effective NHS response system in China is an important issue that my country needs to resolve as soon as possible.

The protocol defines HNS as substances other than oils. If such substances enter the ocean, they may cause harm to human health, destroy biological resources and marine life, pollute the environment, or hinder the legal use of other marine resources. From the definition of the protocol, it can be seen that HNS includes LNG, but due to the hazard characteristics of LNG itself and the specific transportation, the LNG accident response system is different from general toxic and hazardous substances such as

chemicals.

LNG ships and ports are also subject to relevant conventions, regulations, standards, and home and abroad management regulations in terms of safety. The SOLAS Convention requires gas carriers to comply with IGC requirements, shipping companies should maintain a safety management system in accordance with ISM regulations, and ships and ports should take corresponding security measures in accordance with ISPS regulations. The STCW Convention Annex Chapter V lists the outline, operating principles and procedures for the training of tank captains, officers and crews. The United Nations Convention on the Law of the Sea imposes relevant requirements on the supervision and management of port state inspections, manning management of ships, and berthing and operations of foreign ships. The IGC Code is a mandatory regulation on the design, construction and equipment of ships carrying liquefied gas in bulk. It also discusses the unique characteristics of the operation of liquefied gas ships. In addition, relevant industry organizations (SIGGTO, ICS, OCIMF) and others have also formulated LNG ship cargo handling, terminal operations, ship-to-ship transfers, distress contingency plans and crew response, crew training standards, port operations, and safety inspections. Detailed instructions. Various classification societies (BV, DNV, ABS) have formulated detailed rules on the design and construction, classification and certification of LNG ships and offshore terminals. In terms of safety management, the United States, Japan, Australia and other countries have mature management experience, and have formulated management regulations on navigation and other related aspects for LNG ships and ports.

China has also promulgated various laws and regulations to supervise and manage safe production. Various related management regulations promulgated by the Ministry of Transport include ship safety inspection, safety supervision of dangerous goods on

board, waterway transportation of dangerous goods, port dangerous goods management, navigation safety management, ship and port security management, and ship manning management, management of crew watch system and supervision and management of foreign ships. On the technical level, the state has also issued various standards, designing the safe operation of liquefied gas ships, water transfer operations, dock safety, dock design specifications, and statutory inspections of ships and offshore facilities. China Classification Society has also promulgated LNG ship construction and equipment specifications, LNG ship inspection guidelines, and special requirements for special ship inspections. In addition, in the management of LNG ships and crews, the competent authorities at all levels in my country have also formulated various relevant management regulations.

In short, the practice of nearly 50 years has proved that although the risks of LNG maritime transportation and operations are high, the development is relatively mature, and the key is management. As long as the requirements of various conventions, regulations, and standards are carefully implemented, industry risks can be effectively controlled. However, once there is a LNG leakage accident, there are still few relevant technical research reports on how to control the damage of the leaked LNG to the surrounding personnel and facilities. At present, many reports only use fire fighting methods to control the occurrence of fires, but how to set up equipment to reduce the impact of shock waves when LNG boiling, and to control the spread of NG and reduce the area that may cause fires and explosions, are still not recorded in the literatures. This will be a key technology to further ensure the safety of LNG storage and transportation in the future.

1.4 Main contents of the study

Based on the current research status, social development, maritime safety and regulatory needs, this paper adopts numerical research, theoretical analysis and experimental research, combining qualitative analysis and quantitative analysis, and researches on LNG water leakage emergency response mechanism and treatment technology.

(1) Design and build an experimental platform for explosive boiling of LNG releasing on/under water. By changing the LNG composition, releasing pressure, water temperature and water inlet depth, different boiling phenomena can be realized, especially the realization of the explosive boiling phenomenon which is more harmful. In addition to providing different experimental conditions, the experimental system must also fully consider the low-temperature characteristics of LNG and the flammable and explosive characteristics of NG gas produced by boiling.

(2) Visual observation of LNG boiling process. Adopt high-speed dynamic recording and synchronization trigger system (this system can synchronize the triggering of LNG injection time, high-speed dynamic recording time, temperature, and pressure sensor data collection time) to conduct in-depth systematic visual research on the boiling mechanism of LNG, and observe in detail. And record the temperature and pressure vs time.

(3) Establish an emergency response mechanism for LNG carrier leakage accident and a control method for the boiling mode of LNG water area discharge. Development of treatment technology to control boiling rate and change boiling mode, make the

LNG boiling in a stable and gentle manner in the water. So NG can be diluted in a short time and reduce hazard level.

1.5 Research methods and the technical route

1.5.1 Research methods

In view of the complexity of this research problem, it is determined that experimental research must be used as the main method, combined with theoretical analysis and numerical simulation. The central technical route is: to control the LNG components, discharge pressure, discharge port position, nozzle diameter, water temperature and water inlet depth and other experimental conditions based on the dynamic mechanism of LNG water discharge boiling visualization experiment. Use the synchronous trigger system (the system can simultaneously trigger LNG injection time, high-speed dynamic recording time and sensor data collection time), dynamic recording means and real-time temperature and pressure monitoring technology, qualitatively analyze the bubble group morphology characteristics when boiling (including explosive boiling) occurs. Quantitatively analyze the temperature, pressure and mass-heat transfer rate. Analyze the fusion of droplet fragmentation theory, superheat limit temperature theory and in-phase nucleation theory. In order to predict the impact of different emission conditions and surrounding environmental factors on the explosive boiling process of LNG waters, develop calculation software for simulating heat and mass transfer processes under different boiling modes, and improve the qualitative analysis results and boiling theory. Based on the results and the theory of multiphase flow explosion boiling, the control method for limiting LNG boiling in water is proposed. This method is used as an optional module for software simulation and control of boiling mode. The emergency treatment effect is compared and the best

treatment plan is obtained. Summarizing the existing LNG loading and unloading terminal and ship supervision and management status, emergency response mechanism and accident handling technology, based on experimental and numerical results, propose a more scientific and applicable LNG ship leakage emergency response method.

1) Conduct in-depth investigations on various LNG projects, summarize the current LNG loading and unloading docks and ship supervision and management status and emergency response mechanisms, establish an overall technical research plan, and form an overall software function architecture and experimental platform transformation.

2) In the early stage, with the funding of the National Natural Science Foundation of China, I have built an LNG water area discharge experiment platform. The schematic diagram of the experiment system is shown in Figure 1-1.

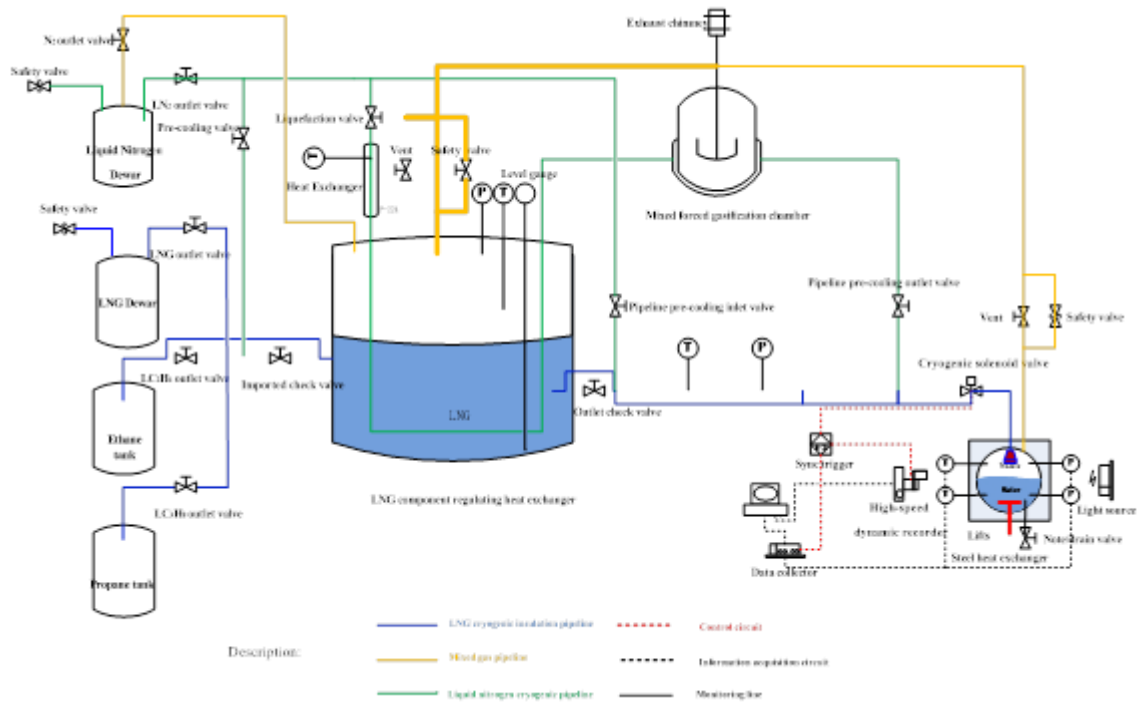


Figure 1-1 Schematic diagram of LNG water area discharge experiment system

Through the above experimental system, it can control the LNG composition, discharge pressure, discharge port position, nozzle diameter, water temperature and the depth of water, and provide experimental basis for the qualitative analysis of LNG boiling mechanism.

3) According to the requirements for visualization of LNG water boiling and pressure and temperature monitoring, the steel heat exchanger in Figure 1 can withstand a pressure of 4 MPa (because the injection volume of the experimental design does not exceed 5 g, the volume of the container is relative to the injection volume. It is much larger, so the 4 MPa withstand pressure can fully meet the experimental requirements. This system is also proved by the applicant's previous LN₂ underwater discharge experiment), and a 25 mm thick acrylic observation mirror is installed on it. This

material has been proven that it can withstand a pressure not less than 4 MPa, and the light transmittance is not less than 92.5%, which can complete the experimental task safely and effectively. At the same time, because multiphase flow boiling is different from the boiling phenomenon with fixed heating walls and high-intensity heat sources, the nucleation interface of the latter is fixed, and the time and mode of boiling are controllable. However, the above two points are not available when the former occurs. Therefore, this research design adopts high-speed camera, temperature and pressure monitoring devices, and LNG injection simultaneously trigger device to synchronize the data recording with the experimental process. The pressure and temperature signals obtained by monitoring are sampled and saved by the data acquisition instrument, and the pressure change rate data is calculated. The mass transfer and heat transfer rate calculation model is used to obtain the boiling heat flux between water and LNG, and then use numerical models to simulate the temperature rise rate of LNG under this heat flux condition, which is used as the determining condition for the boiling mode judgment, that is, different temperature rise rates represent different boiling modes. On this basis, by changing the experimental conditions, the purpose of controlling the intensity of boiling is achieved, so that the leaked LNG liquid will boil in a stable and gentle manner in the water, providing an experimental and theoretical basis for the development of LNG leakage emergency treatment technology.

4) Since the boiling characteristics of multiphase flow are obviously relatively simple and lacking sufficient convincing analysis only from the perspective of temperature rise rate, after 2) the boiling mode is determined, the high-speed dynamic recording images are played back to carefully analyze the boiling characteristics. The behavioral characteristics of the bubble group, clarify the influence of the micro-time scale effect of the basic internal processes of boiling, such as nucleation, growth, detachment, merging and floating of bubbles, on the overall boiling process, and in-depth

exploration and reveal the law of the influence of various experimental conditions on the bubble evolution process, and strive to reveal the transformation process of LNG water boiling mode in a more in-depth mechanism.

5) Based on the experimental results of dynamic mechanism and multiphase flow explosion boiling theory, in order to predict the decisive effect of different emission conditions and surrounding environmental factors on the boiling mode transition, software was developed to simulate this process. The software can determine the boiling mode of the LNG leakage process by setting the emission conditions and environmental factors, and calculate the area affected by the expansion of the liquid pool and the diffusion of NG gas during the boiling process. In addition, optional post-treatment measures are provided in the software to compare the LNG leakage process after the emergency treatment of the accident with the untreated leakage, and analyze the best treatment method.

6) Based on the LNG water area discharge experimental data and theoretical analysis, a more scientific and suitable LNG ship water area leakage emergency response is proposed. The relevant suggestions and specific measures of the mechanism provide theoretical basis and technical reserves for the safe storage and transportation of LNG.

1.5.2 Technical route

The technical route of this paper is shown in Figure 1-2.

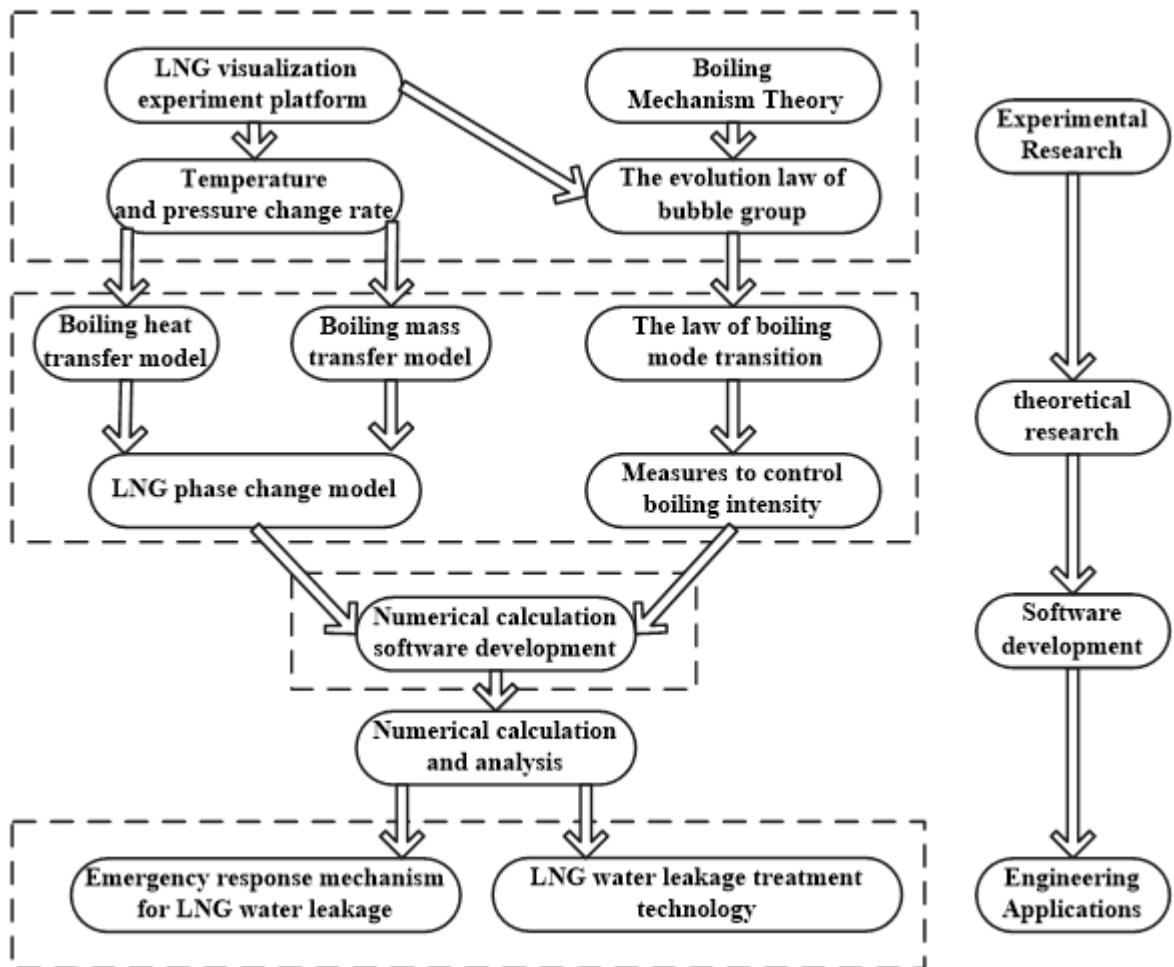


Figure 1-2 Technical roadmap of the research

Chapter 2 Experimental research

2.1 Experimental apparatus

The experimental rig (Figure 1-1 and Figure 2-1) consists of a condensation system, a mixer tank, an injector, a visualized pressure tank (Fig. 1(c)), and a data acquisition system.

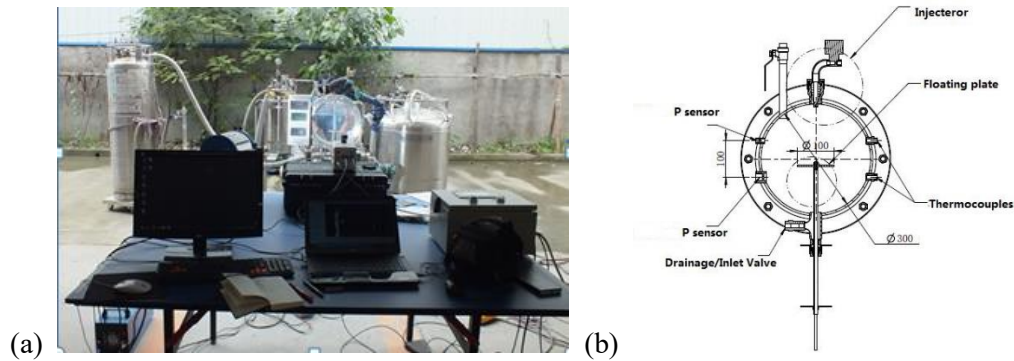


Figure 2-1 Experimental system and apparatus: (a) picture of apparatus; (b) positions of all sensors in tank.

LN₂ and LNG are separately delivered through insulated pipe and outlet valve from a controllable pressure Dewar. Out of necessity, LNG injection must occur below its bubbling point, which can be conducted in the LNG mixer tank by LN₂. After the LN₂ delivered through LNG mixer tank, the temperature of LNG in mixer tank can be maintained at 100K(±5K), that is ~10K below the LNG bubbling point. The pressure of LNG mixer tank equals to injection pressure, which is controlled by manually adjusting the pressure regular valve on LN₂ Dewar. Because the propane gas is storage

¹ The research of this Chapter has been published on the journal of Applied Ecology and Environmental Research. "Bin ZHANG*, Xingdong Zhang, Wanqing Wu. Experimental Study on Cryogen Injection into Water[J]. Applied Ecology and Environmental Research, 2017, 15(4): 441-456."

in the gaseous phase, before injecting, it must be condensed into liquefied propane, which can be conducted in a similar way like LNG cooling process. In the LN₂ injection process, the system must be improved and the LN₂ Dewar outlet valve to be directly combined with the mixer outlet valve. Where after, the cryogen liquid is delivered to an ASCO intrinsically safe type cryogenic solenoid valve, which controls the opening of the injector. The injector is made of a 25mm length of steel pipe with an inside diameter of 5mm. To prevent heat leakage, the all cryogenic liquid pipes are made of double insulated vacuum steel pipe, and before experiments, the pipes are precooled by LN₂ and the time is not less than 10 min.

The visualized pressure tank is a stainless cylinder of diameter 300mm and depth 150mm with Perspex windows clamped onto each end. The safety valve and vent valve are fitted on the tank to prevent pressurization above 40 bars and can vent the vapor respectively. Two T-type sheathed thermocouples of 10mm in diameter, 140mm in length, with accuracy of 0.5% FS and two high frequency dynamic pressure sensors of 4mm in diameter, 10mm in length, with accuracy of 0.5% FS with minimum response time of 4 μ s are used to measure the temperatures and pressure within the tank. The positions of all sensors are illustrated in Fig. 1(c).

The boiling process of LNG into water is recorded by a high speed camera (Svsi Gigaview) with the frame rate of 532~17045 frames per second. In this series experiments, the frame rate is 1000 frames per second, and frame size is 640 \times 480 pixels. A 575 W quartz metal halide light source is added to improve the qualities of the frames. The camera and the image acquisition software are triggered by the leading edge of a 5 V pulse generated within PLC (Programmable Logic Controller) hardware, programmed and controlled by the operator. The image acquisition software comes with the camera and can set the image acquisition rate, image pixel and exposure time.

The same pulse triggers the National Instruments Data-Acquisition hardware and LabVIEW to acquire and store both pressure and temperature data, at a rate of 10,000 samples per second. Another 5V pulse is generated after 100 ms within the PLC, which is used to trigger the ASCO solenoid valve opening. The opening time is dependent on the trigger pulse width, which can be set manually within the PLC.

2.2 Experimental results

Table 2-1 Experiment run parameters

Run	Component Concentration CH ₄ :C ₂ H ₆ : C ₃ H ₈ :OS (v/v %)	Water Temperature (K)	Floating Plate Location under Water (mm)	Injection Pressure (Bar)	Injection During time (ms)	Max. Pressure (Bar)	Max. Pressure Occurring Time after Injection (ms)
1	97 : 2 : 0.5 : 0.5	290	210	7	200	3.01	6553
2	97 : 2 : 0.5 : 0.5	290	140	7	200	1.61	6284
3	97 : 2 : 0.5 : 0.5	290	210	5	200	1.64	5558
4	97 : 2 : 0.5 : 0.5	308	140	7	200	1.00	6442
5	C ₃ H ₈ : 100%	303	200	4	300	0.23	12465
6	OS: 100%N ₂	290	210	7	200	2.44	5946

By controlling the LN₂ Dewar outlet pressure and outflow, the different injection pressures and thermodynamic states of cryogen can be adjusted. A number of cryogen injection experiments are conducted, of LNG, LN₂ and LC₃H₈, into water of different temperature and depth. The parameters for experiments are shown in Table 1. The LNG component concentration is provided by the LNG supplying company. By adjusting the location of floating plate under water, the cryogen injection into water depth can be controlled. Injecting during time can be controlled by the power time of ASCO solenoid valve.

2.3 Analysis of the experimental results

2.3.1 Heat transferring flux

As Table 1 shown, the maximum pressure occurs in run 1, which injection pressure is one of the highest, water temperature is one of the lowest and floating plate location under water is bottommost. The pressure of the visualized pressure tank is shown in Figure 2-2(a) over a 10 s timescale and additionally in Figure 2-2(b) for the maximum pressure occurring time over 100 ms timescale (from 5400 ms to 5499 ms after injection). In Figure 2(a), the pressure data is recorded by the high frequency dynamic pressure sensors of 10 mm in length, before trigger activating 100 ms. In Figure 2(b), the pressurization is extremely rapid at ~ 300 bar/s. Using TNT equivalent model can simplify the process so that the heat transfer coefficient can be obtained. The following expressions relating the maximum pressure and the heat transfer flux.

$$W_{TNT} = k \frac{aW_{LNG}Q_{LNG}}{Q_{TNT}} \quad (2.1)$$

$$\Delta P = P_0(3.9Z^{-1.82} + 0.5Z^{-1}) \quad (2.2)$$

$$Z = R \cdot W_{TNT}^{-1/3} \quad (2.3)$$

$$H_{RPT} = L_V \cdot W_{LNG} / (S \cdot t_d) \quad (2.4)$$

Where W_{TNT} is TNT equivalent, kg; W_{LNG} is LNG mass which is fragmented, kg; k is surface burst coefficient; a is equivalent coefficient; Q_{LNG} is bursting heat, J; Q_{TNT} is TNT bursting heat, J; ΔP is maximum pressure value, Pa; R is distance from pressure sensor, m; H_{RPT} is heat transfer flux, of explosion boiling W/m^2 ; L_V is latent heat of LNG, J/kg; t_d is the duration time of pressure increasing, s. It is ~ 10 ms obtained from

the Figure 2-2. Combining Eqs. (2.1)-(2.4), the maximum heat transferring flux can be over 1.9 MW/m^2 . It is ~ 7.8 times bigger than the theoretical limit of heat transferring flux of the pure liquefied methane nucleate boiling (0.244 MW/m^2).

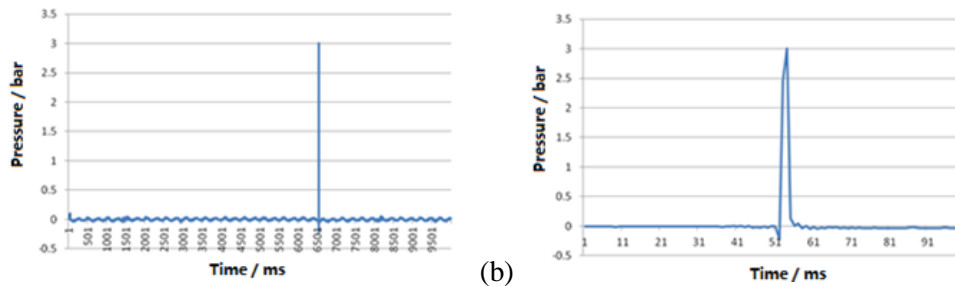


Figure 2-2 Pressure curve correspondent to run 1 using the P sensor under water: (a) the time is from 0 ms to 10000 ms after injection; (b) the time is from 5400 ms to 5499 ms after injection).

2.3.2 Theoretical analysis about instability

As cryogen injecting into water, the interface between cryogen and water would be with wave. If disturbances of all wavelengths are present, there will be some disturbances at small wave number and long wavelength that will amplify and cause the interface to be unstable. There are four main instability theories can be used to explain the explosive boiling mechanism of cryogen injection into water.

(a) Rayleigh-Taylor instability(BYOUNG J. K.;2015)

It is the instability of an interface between two fluids of different densities which occurs when the lighter fluid is pushing the heavier fluid. If the energy of interface tension is higher than the sum of kinetic energy of fluctuations and potential energy, the interface will be with a stable vapor film. Otherwise, the interface will be unstable and the vapor film will be broken because of the Rayleigh-Taylor instability. It takes more effect on the leading end than the side of liquid column. The most dangerous

wavelength is given by

$$\lambda_D = 2\pi \sqrt{\frac{3\sigma}{|\rho_{cl} - \rho_w|g}} \quad (2.5)$$

Where λ_D is the most dangerous wavelength, m; ρ_{cl} is liquid cryogen density, kg/m³; ρ_w is circumstance fluid density, kg/m³; σ is the interfacial tension, N/m; g is the gravitational acceleration, m/s².

(b) Kelvin-Helmholtz instability(HYUN G. L.;2015)

When there is a sufficiently large velocity difference across a small amplitude perturbed interface between two fluids, the interface is unstable. This interfacial instability is known as the Kelvin-Helmholtz instability. The instability occurs when the destabilizing effect of shear across the interface overcomes the stabilizing effect of gravity and/or surface tension. It takes obvious effect on the side of liquid column. If a specific disturbance wavelength is imposed on the system, the interface will be unstable for

$$|\overline{u_{cl}} - \overline{u_w}| > u_c \quad (2.6)$$

$$u_c = \sqrt{\frac{2\pi\sigma(\rho_{cl} + \rho_w)}{\lambda_D\rho_{cl}\rho_w} + \frac{g\lambda_D(\rho_{cl} - \rho_w)(\rho_{cl} + \rho_w)}{2\pi\rho_{cl}\rho_w}} \quad (2.7)$$

If g is set to zero, we get the dispersion relation for a vertical interface, which implies that

$$u_c = \sqrt{\frac{2\pi\sigma(\rho_{cl} + \rho_w)}{\lambda_D \rho_{cl} \rho_w}} \quad (2.8)$$

The most dangerous wavelength is given by

$$\lambda_D = \frac{2\pi\sigma(\rho_{cl} + \rho_w)}{u_c^2 \rho_{cl} \rho_w} \quad (2.9)$$

Where u_c is critical velocity, m/s; u_{cl} is liquid cryogens velocity, m/s; u_w is circumstance fluid velocity, m/s.

(c) Weber number

As cryogen injecting into water, the velocity difference between the two fluids will produce tangential stress on the interface. If the tangential stress is bigger than the surface tension, the cryogen column will be broken into liquid droplets. The minimum diameter of stable liquid droplets is dependent on the magnitude of shear stress, which will be increased with the velocity difference increasing. The minimum characteristic length of stable liquid column or droplets is given by

$$L = \frac{We_c \sigma}{\rho_w (u_{cl} - u_w)^2} \quad (2.10)$$

$$We_c = \frac{8}{f} \quad (2.11)$$

Where L is minimum characteristic length of stable liquid column or droplets, m; We_c is critical Weber number; f is friction coefficient, $f=0.44$ when $500 < Re < 105$.

(c) Marangoni effect(TANG, 2013)

Marangoni effect is caused by the heterogeneity of the surface tension near interface of two fluids with different temperature. In subcooled flow boiling, the surface tension gradient along two fluids contact interface is raised from the temperature difference in the vapor film around the liquid cryogen column, which leads to the tangential stresses of τ_{cl} and τ_{cv} on liquid cryogen side and vapor cryogen side at the interface respectively. Due to reaction of the stresses of τ_{cl} and τ_{cv} , the liquid and vapor phase of cryogen were accelerated and the Marangoni effect formed near the interface. Figure 2-3 shows a schematic diagram to describe the Marangoni effect near a smooth and stable vapor film caused by temperature gradient and the force balance in tangential direction on the cryogen surface. Under steady state condition, the balance of forces at the interface is

$$\tau_{cl} + \tau_{cv} = \frac{d\sigma}{dT} \frac{\Delta T}{\delta} \quad (2.12)$$

Moreover, the shear stress on vapor side at the interface τ_{cv} can be neglected since the most gases viscosity is much smaller. Therefore, the simplification of Eq (2.12) is

$$\tau_{cl} = \frac{d\sigma}{dT} \frac{\Delta T}{\delta} \quad (2.13)$$

Strength of Marangoni effect can be characterized by the Marangoni number

$$Ma = \left| \frac{\tau_{cl} \delta^2}{\alpha_{cl} \mu_{cl}} \right| \quad (2.14)$$

Where τ_{cl} is shear stress on liquid side, N/m²; τ_{cv} is shear stress on vapor side, N/m²; δ is the characteristic length of interface, m; α_{cl} is thermal diffusivity of cryogen liquid, m²/s; μ_{cl} is the dynamic viscosity of cryogen liquid, kg/s•m.

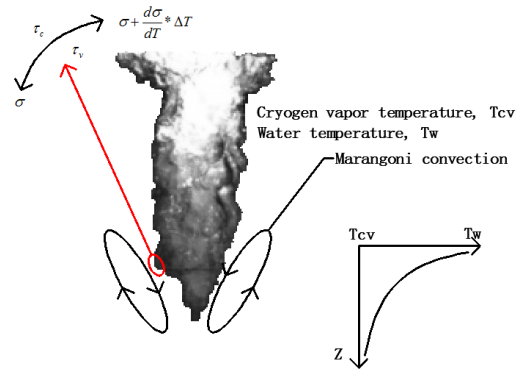


Figure 2-3 Schematic diagram of Marangoni convection near the vapor film (The original image is 3d in Figure 2-5)

2.3.3 Effect of injection depth into water

Comparing run 1 and run 2, the maximum pressure of run 2 decreases $\sim 46.5\%$, and the time of maximum pressure occurs $\sim 270\text{ms}$ ahead. Besides the location of floating plate, the other parameters of experiments are similar. As a result of that, the mainly reason for the differences between the two runs is the depth of injection into water. According to the Kelvin-Helmholtz instability and critical Weber number theory, as Eq (2.6) is satisfied, the interface between cryogen and water will become unstable and the liquid column of cryogen will be broken into small droplets, which diameter is equal to the λ_D or L is separately calculated by Eq(2.9) and Eq(2.10). The effective heat transferring area is remarkably increasing. But if the liquid column of cryogen impinges the floating plate, $|\overline{u_{cl}} - \overline{u_w}|$ will be reduced to zero, liquid column of cryogen stop breaking into droplets in the effect of instability. But the collision process will become complicated. The droplets of cryogen may be undergone two contradicting processes that are coalescence and breakup. The maximum pressure of run 2 is lower than run 1, it implies that the coalescence effect in the collision process has an obvious effect, that can decrease the heat transferring capacity and boiling rate. From another point of view,

because the injection depth into water is unconfined, the breakup during time of liquid droplets or column in run 1 is longer than run 2 which induces the maximum pressure occurring time being aback.

As a result, as cryogen releasing or injecting into water, the maximum pressure or boiling rate will be reduced by confining the water depth, which can be used to limit explosive boiling occurring.

2.3.4 Effect of injection pressure

Comparing run 1 and run 3, the $\overline{u_{cl}}$ in run 3 is smaller than run 1, as a result, the maximum pressure of run 3 is ~45.5% smaller than run 1. It implies the heat transfer capacity and boiling rate of run 3 are both smaller than run 1. There are two main reasons for the difference of the maximum pressure. Firstly, in the effect of Kelvin-Helmholtz instability, as Eq(2.6) is satisfied, the liquid column of cryogen will breakup into droplets, and the mean diameter of droplets is equal to the most dangerous wavelength λ_D , which will be reduced with $|\overline{u_{cl}} - \overline{u_w}|$ increasing. Secondly, basing on the Weber number theory, as $|\overline{u_{cl}} - \overline{u_w}|$ increasing, the tangential stress on the interface will increase, which will decrease the minimum characteristic length L that means the liquid droplets will break into much smaller droplets. The heat transferring area will dramatically increase, which implies both boiling rate and heat transferring capacity will substantial increase.

Furthermore, the occurring time of maximum pressure is ~1000ms earlier than run 1. It means the breakup duration time of liquid column and droplets of cryogen in run 3

is shorter than run 1. In another word, the time of liquid column and droplets stopping breaking into smaller diameter droplets in run 3 is earlier than run 1.

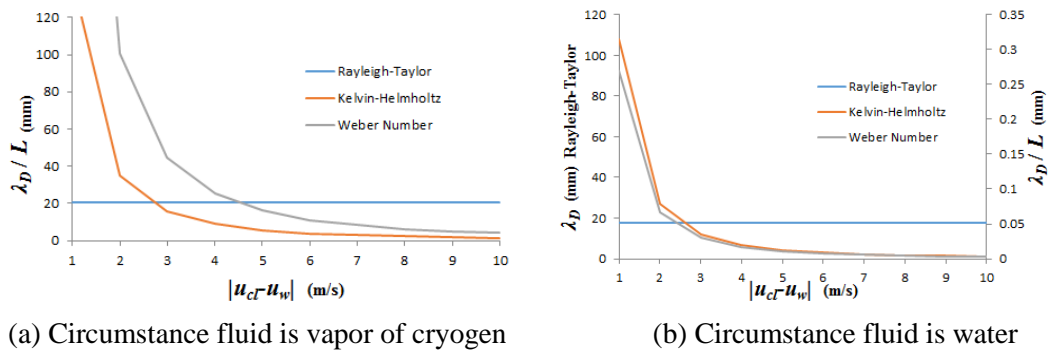
In conclusion, the injection pressure is related to the boiling rate. As the injection pressure increasing, the maximum pressure will increase and its occurring time will be advanced, which will increase the probability of explosive boiling.

2.3.5 Effect of water temperature

Comparing run 2 and run 4, the water temperature of run 4 is higher than run 2, as a result of that the maximum pressure of run 4 is ~37.8% smaller than run 2. Figure 2-4a shows the circumstance fluid is vapor film, whose temperature is equal to the water temperature of run 2. There is a hypothesis the water temperature is low enough that there is no evaporation occurring, so the circumstance fluid is water as the Figure 2-4b showing. Both the most dangerous wavelengths in Rayleigh-Taylor instability in Figure 2-4 are approximately equal. But the most dangerous wavelengths in Kelvin-Helmholtz instability and the minimum characteristic lengths in Weber Number theory in Figure 2-4 varies greatly. It implies, as the concentration of vapor in the interface between cryogen and water decreasing, the most dangerous wavelengths in Kelvin-Helmholtz instability and the minimum characteristic lengths in Weber Number theory dramatically decreasing, which intensifies the cryogen column and droplets breaking up into much smaller droplets and promotes higher heat transferring rate and boiling intensity.

Furthermore, the maximum pressure occurring time of run 4 is a little bit later than run 2. That is because, as the water temperature increasing, the initial film boiling rate and

vapor film thickness in run 4 are separately higher than run 2, which will decrease relative velocity and the instability effects of the interface, as a result of that it needs much more time to trigger cryogenic column breaking into droplets and dramatically decreasing heat transferring capacity.



(a) Circumstance fluid is vapor of cryogen (b) Circumstance fluid is water
 Figure 2-4 Most dangerous wavelength in Rayleigh-Taylor instability and Kelvin-Helmholtz instability, and minimum characteristic length in Weber Number Theory

As a result, if the water temperature is increasing, the instability of Kelvin-Helmholtz and Weber number will be reduced. The diameter of droplets breaking from column will be increased. The effective area of heat transferring will be considerably decreased, which will reduce the heat transferring capacity and have less opportunity to trigger explosive boiling.

Base on the thermodynamics theory, if the temperature of water is higher than Leidenfrost temperature of cryogen (VAN P.C.;1992), there will be a film boiling. The Leidenfrost temperature for methane, ethane, propane and nitrogen are 161K, 249K, 312K and 126K, respectively. And only if the water temperature is equal or slightly greater than the superheat limit temperature of cryogen ($T_{\text{superheat}} < T_{\text{water}} < 1.1 T_{\text{superheat}}$), the explosive boiling will be triggered(LUKETA-HANLIN ,2006). The superheat limit temperature for methane, ethane, propane and nitrogen are 168K, 269K, 326K and

110K, respectively. But the water temperature is not the only factor for triggering explosive boiling. Because, in run 1, run 2 and run 3, it has the same condition of water, the maximum pressures have great differences. There should be some other factors for triggering explosive boiling, such as injection pressure, injection depth into water and working substances.

2.3.6 Effect of injecting cryogen

From Table 1, the run 1, 5 and 6 are separately used LNG, LC_3H_8 and LN_2 . It shows that the maximum pressure of run 1 is ~18.9% bigger than run 6, and ~13 times of run 5. Furthermore, the maximum pressure occurring time of run 6 is earlier than run 1, and much earlier than run 5. There are three main reasons.

(1) LNG is mixture. In the process of LNG injecting, the LNG column will be heated by surrounding water and some of it will boil into vapor phase. As a result of that, liquid LNG components will change and bubble point changes correspondingly. On the effect of Marangoni effect, the surface tension gradient along two fluids contact interface is raised from the bubble point difference in the vapor film around the liquid cryogen column, which leads to the tangential stresses. If the tangential stress is bigger than the surface tension, the cryogen column will be broken into liquid droplets or big droplets further break into small ones. But LC_3H_8 and LN_2 are both pure substances whose boiling temperatures only relate to the pressure. So the surface tension gradient along two fluids contact interface is raised from the initial degree of subcooling. In run 6, the LN_2 is nearly saturation liquid, so there should be less Marangoni effect in this process. In run 5, the LC_3H_8 has ~120 degrees of subcooling, so there should be an obvious Marangoni effect. That can be seen from the Figure 2-5. Comparing 1a~1f

and 2a~2f, the pattern of LNG bubbles have a less value of L_c/D_c than LN_2 bubbles (L_c is the length of the bubbles pattern; D_c is the diameter of the bubbles pattern). It means LNG column suffers much more tangential stress than the LN_2 , which makes more bubbles break up from side than the leading end. And from 3a~3f, the LC_3H_8 bubbles generate more from side than the leading end of liquid column. It means the Kelvin-Helmholtz instability and Marangoni convection occupies leading position on the process of column breaking into droplets.

(2) The degrees of subcooling of LC_3H_8 is much more than LNG and LN_2 , as a result of that, it needs more time and heat to be saturated, and in turn, the maximum pressure occurring time of run 5 (LC_3H_8) is obviously later than the other runs of 1 (LNG) and 6 (LN_2). Furthermore, the maximum pressure occurring time of run 1 is a little later than run 6. On one side, the density of LNG is less than LN_2 , which causes the relative velocity of LNG is slower than LN_2 . On the effect of instabilities of Kelvin-Helmholtz and critical Weber number, the intensity of breaking of LNG is not as strong as LN_2 . So the maximum pressure occurring time of LNG is not as early as LN_2 . On the other side, the LNG is subcooling cryogen and the LN_2 is saturate substance. In the process of LNG injection, it needs some time to heat it to be saturated, though the time will be substantially short as the difference of temperatures of LNG and water being huge.

(3) From the above analysis, the Marangoni convection has an obvious effect on strengthen heat transferring rate. Base on the instabilities of Rayleigh-Taylor, Kelvin-Helmholtz and critical Weber number theory, the maximum pressure detected in LN_2 test (run 6) should be higher than LNG test (run 1). But the real results are just the opposite. The mainly reason is the effect of Marangoni effect. As the relative velocity becoming slower and slower, the Marangoni convection takes the leading position and the instability effects of Rayleigh-Taylor, Kelvin-Helmholtz and critical Weber

number theory becomes weaker and weaker. Because of the effect of Marangoni convection prolonging the breaking time of droplets, the maximum pressure and the occurring time of maximum pressure in run 1 is separately higher and later than run 6.

2.3.7 Bubble behaviors analysis

From these images of 1a~1f and 2a~2f in Figure 2-5, the structure and pattern of bubbles have a similar developing process in run 1 and run 6. It can be characterized in three main stages.

(1) Stable film boiling stage: from the images of 1a~1b and 2a~2b, it can be seen that liquid cryogen flashes as it impinges into water and forms a vapor void. Because the injection process is likely to continue for some time, the following liquid cryogen is injected into the void created by the former boiling cryogen. A velocity difference forms on the relatively stable vapor film between liquid cryogen and water, but the water outside vapor film is nearly static. So the liquid cryogen inside vapor film is moving downwards under a high speed. There is no significant breaking on the liquid cryogen column, although formation of waves on the vapor film due to the instability of dynamics is observed.

(2) Bubbles cloud generation stage: as the liquid cryogen continuously moving downwards, on the effect of instabilities of Rayleigh-Taylor, Kelvin-Helmholtz and critical Weber number, the shearing stress is bigger than the surface tension, and then the ligaments and fragmentations take place. In the images of 1c~1d and 2c~2d, it shows the vapor film becomes thinner and lighter. There is a cloud of bubbles form on the head and the side of the column (WEN,2006). The cloud of bubbles is extremely

unstable; some of them will be coalescence and others will be continuously breaking up into smaller ones. The heat transferring rate will be dramatically increasing as a result of the bubbles growing up and breaking which enhances the heat convection between cryogen and water. On the effect of Marangoni convection, the images of 1c~1d show the bubbles cloud has a more unstable vapor film nearby the head of column than 2c~2d.

(3) Buoyancy taking over stage: in the images of 1e~1f and 2e~2f, it shows that, in the last stage of injections, the buoyancy force will take over. The bubbles cloud gradually disappears and forms much bigger bubbles that are so stable that they cannot be broken up again in the upwards moving process. Comparing the images of 1e~1f and 2e~2f, the bubbles cloud maintains longer in run1, because of the effect of Marangoni convection.

The images of 3a~3f in Figure 2-5 shows a different structure and pattern of bubbles. It can be characterized in two main stages.

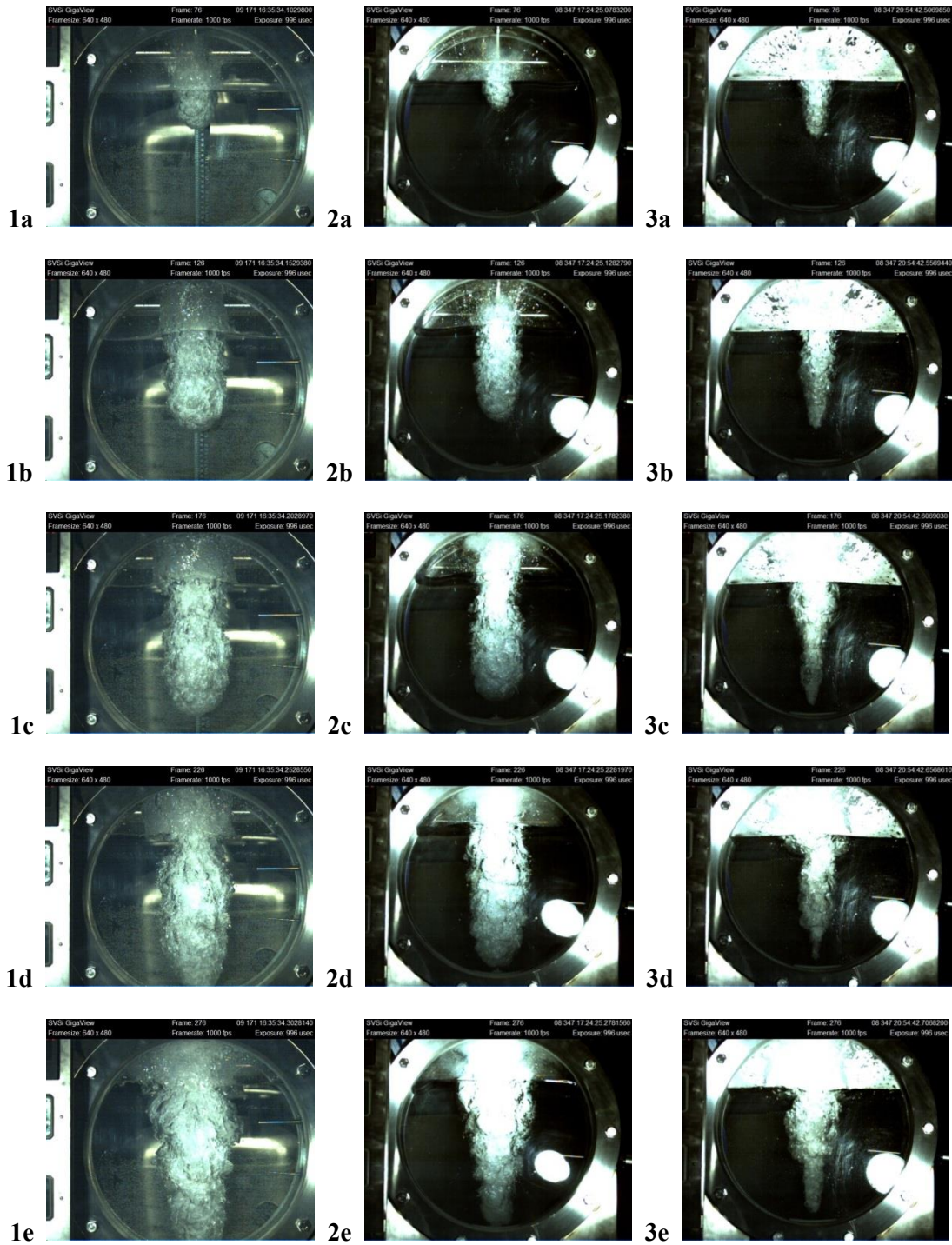
(1) Stable flow boiling stage: in all images of run 5, the LC_3H_8 column has a relatively obvious shape and the boiling is not as violent as run 1 and 5. Most of it has no significant breaking except the periphery of the vapor film near the head of column in the image of 3d. There are three main reasons.

Firstly, the water temperature is $\sim 303K$, which is less than the superheat limit temperature of LC_3H_8 . As a result of that, the explosive boiling would have less opportunity to take place and it undergoes a relatively stable boiling, that is subcooled flow boiling.

Secondly, because of the ~ 120 degrees of subcooling, after LC_3H_8 injecting into water, it needs much more time to be heated to the saturate temperature by surrounding water. As a result of that, it can maintain an obvious liquid column shape in a relative long time. Because the water temperature is less than the Leidenfrost temperature of LC_3H_8 , the vapor film of run 6 is not as stable as run 1 and 5, and the surrounding fluid will be water. The relative velocity, which is related to density difference between LC_3H_8 and surrounding fluid, is less than run 1 and 6. Basing on the instability of Kelvin-Helmholtz and Weber number, as relative velocity decreasing, the most dangerous wavelength and minimum characteristic length will be considerably increasing. It implies the LC_3H_8 will become more and more stable and suffer less from the instability of Kelvin-Helmholtz and Weber number.

Finally, LC_3H_8 is ~ 120 degrees of subcooling. As a result, in subcooled flow boiling, the surface tension gradient along two fluids contact interface is raised from the temperature difference in the vapor film around the liquid cryogen column, which leads to the tangential stresses on liquid cryogen side and vapor cryogen side at the interface respectively. When the stresses accrete to higher than the surface tension, the Marangoni effect will take place and some of the liquid column will breakup into small droplets, which can be seen in the image of 3d. From that image, we can also know that the periphery of the vapor film near the head of column is considerably stronger than other regions in the effect of Marangoni.

(2) Buoyancy taking over stage: in the images of 3e~3f, it shows that, in the last stage of injections, the buoyancy force will take over. The evaporating bubbles move upwards in a higher speed than the LC_3H_8 column and begin to separate from it. After that, the LC_3H_8 column still staying in the water is not broken again and some of it maintains liquid phase until floating on the water and forms liquid pool.



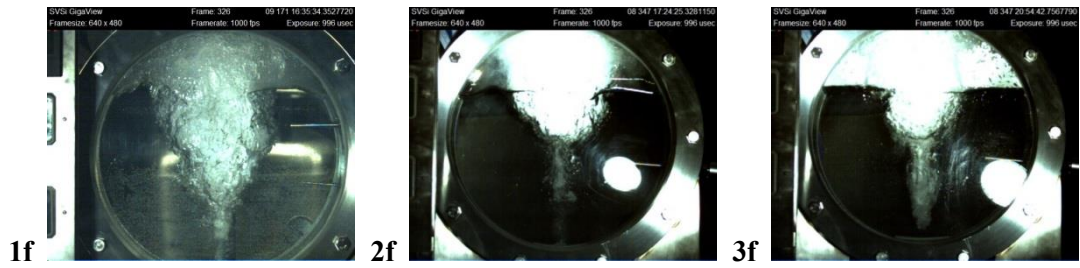


Figure 2-5 Bubble behaviors of cryogen injection into water (1a~1f are images of run 1, 2a~2f are images of run 6, 3a~3f are images of run 5. The interval time between the adjacent two images is 50 ms).

²Chapter 3 Numerical research

LNG releasing on/under sea will cause a number of boiling styles, such as film boiling, transition boiling, nucleate boiling and even explosive boiling. In the Chapter 2, the LNG boiling process has been analyzed. Beside boiling process, the releasing process includes LNG spreading and NG dispersion. In this Chapter, the numerical models will be built up to simulate the whole releasing process.

3.1 Numerical models

(1) Releasing rate

For liquids flowing through an orifice the Bernoulli equation can be applied. Neglecting the initial liquid velocity in the carrier, the mass flow rate can be estimated by

$$S(t) = C_d A \rho_l \left[\frac{2(P-P_a)}{\rho_l} + 2gh_h(t) - 2g \frac{m_{ejection}(t)}{\rho_l A_T} \right]^{\frac{1}{2}} \quad (3.1)$$

Where S is mass flow rate, kg/s; t is time, s; A is cross-section area of the hole, m^2 ; A_T is cross-section area of releasing tank, m^2 ; ρ_l is liquid density in releasing tank, kg/m^3 ; P is storing pressure in releasing tank, Pa; P_a is atmospheric pressure, Pa; h_h is liquid height above hole in the releasing tank, m; $m_{ejection}$ is the mass flow rate of ejection

² The research of this Chapter has been published on 4th International Conference on Information Science and Control Engineering. “**Bin ZHANG***, Xingdong Zhang, Wanqing Wu. Numerical Study on LNG Carrier Releasing Underwater and Emergency Treatments[C]. 4th International Conference on Information Science and Control Engineering. 2017.7.21-2017.7.23”

system, kg/s. C_d is discharge coefficient.

(2) Spreading on water

The radius of the pool for spreading on water is given by

$$\frac{d^2 r}{dt^2} = \frac{du_p}{dt} = \frac{4 \times \varphi(t) \times g \times (\rho_w - \rho_l(t)) \times h_{pool}(t)}{r(t) \times \rho_w} - D(t) \quad (3.2)$$

here subscription l and w is specifically LNG and water; r is pool radius, m; h_{pool} is pool thickness, m; ρ is density, kg/m³; j and φ are both gravity coefficient; u_p is pool spreading speed, m/s; D is resistance coefficient, m/s².

(3) Heat and mass transfer

The conservation of energy, neglecting all mechanical friction terms, applied to an evaporation pool, is given by

$$Q_{net} = Q_{spill} + Q_{sub} + Q_{air} + Q_{rad} + Q_{treat} - Q_{evap} \quad (3.3)$$

$$\frac{dT_l}{dt} = \frac{Q_{net}(t)}{m_{pool}(t)c_{pl}(T_l)} \quad (3.4)$$

$$Q_{spill} = S(t) \{c_{pl}(T_{il})[T_{il} - 273] - c_{pl}(T_l)[T_l - 273]\} \quad (3.5)$$

$$Q_{air} = h_a \pi r(t)^2 (T_a - T_l(t)) \quad (3.6)$$

$$Q_{rad} = S_s \pi r(t)^2 + 5.386 \times 10^{-8} (T_a^4 - T_l^4(t)) \quad (3.7)$$

$$Q_{treat} = h_{treat} \pi r(t)^2 (T_{treat} - T_l(t)) \quad (3.8)$$

$$Q_{evap} = \pi r(t)^2 U_a^* D a^* h_{lg} \frac{\bar{M}}{RT_l(t)} \ln \left(\frac{P_a}{P_a - P_v^s(T_l)} \right) \quad (3.9)$$

$$Q_{sub} = h_{sub} \pi r(t)^2 \quad (3.10)$$

$$h_{sub} = h_{fb} = \begin{cases} 0.62 \left\{ \left[\frac{k_v^3 g(\rho_l - \rho_v) \rho_v h_{lg}}{\mu_v(T_w - T_{sat}) d_l} \right] \left[1.0 + \frac{0.4 c_{pv}(T_w - T_{sat})}{h_{lg}} \right] \right\}^{\frac{1}{4}} (T_w - T_{sat}) \\ \text{for underwater} \\ 1.29 \left\{ \left[\frac{k_v^3 g(\rho_l - \rho_v) \rho_v h_{lg}}{\mu_v(T_w - T_{sat})} \right] \left[\frac{g(\rho_l - \rho_v)}{\sigma_v} \right]^{\frac{1}{2}} \right\}^{\frac{1}{4}} (T_w - T_{sat}) \\ \text{for onwater} \end{cases} \quad (3.11)$$

There is a hypothesis that only thermodynamic instability triggers explosive boiling in the process of LNG releasing underwater. Because LNG is mixture, the bubble point will be changed with the changing of LNG components concentration. If $1.1 T_{SLT} > T_w > T_{SLT}$ and $T_w < T_c$ then there may be explosive boiling, and the heat transfer flux is

$$Q_{sub} = Q_{eb} = \frac{2h_{lg}}{2 - K_c} \left(\frac{\bar{M}}{\pi d_l} \right)^{1/2} \left(\frac{K_c P_v}{T_v^{0.5}} - \frac{K_e P_l}{T_l^{0.5}} \right) \quad (3.11)$$

If $T_w < T_{leidenfrost}$ then there may be transition boiling, and the heat transfer flux is

$$h_{tb} = \left(0.09 f \rho_v h_{lg} \left[\frac{g(\rho_l - \rho_v) \sigma_v}{(\rho_l + \rho_v)^2} \right]^{\frac{1}{4}} + 0.16 (-f) \rho_v h_{lg} \left[\frac{g(\rho_l - \rho_v) \sigma_v}{\rho_v^2} \right]^{\frac{1}{4}} \right) (T_w - T_{sat}) \quad (3.12)$$

The mass transfer coefficient from LNG to NG is

$$m_{lv} = \frac{Q_{net}}{h_{lg} + c_{pl}(T_{sat} - T_l)} \quad (3.13)$$

Where Q_{net} is total heat, W; Q_{spill} is liquid heat, W; Q_{sub} is convection heat from water, W; Q_{air} is convection heat from air, W; Q_{rad} is solar radiated heat, W; Q_{treat} is convection heat from emergency treatment, W; Q_{evap} is evaporation heat form liquid, W. ; T_{il} is LNG initial temperature, K; m_{pool} is pool mass, kg; c_p is specific heat, J/(kg·K); $c_{\text{pl}}(T_1)$ is LNG special heat in T1, J/(kg·K); T is temperature, K; h_a is air convection heat transfer coefficient, W/(m²·K); S_s is solar radiation heat transfer flux, W/m²; h_{treat} is emergency treatment convection heat transfer coefficient, W/(m²·K); T_{treat} is emergency treatment substance initial temperature, K; M molecular-weight average, g/mol; h_{lg} is latent heat of vaporization, J/kg; U_a^* , is pool moving velocity on the effect of air velocity, =0.045 u_a ($z=10$ m), m/s; Da^* is Dalton number; $P_{\text{vc}}(T_1)$ is saturated vapor pressure in T_1 , Pa; h_{sub} is heat transfer flux from water, W/m²; $T_{\text{leidenfrost}}$ is Leidenfrost temperature of LNG, K; T_C is critical temperature of LNG, K; T_{SLT} is superheat limit temperature of LNG, K. $T_{\text{leidenfrost}}$, T_C and T_{SLT} of LNG are approximately the mole fraction average of them of the components, and their values are shown in Table 3-1. h_{fb} is film boiling heat transfer flux, W/m²; k is thermal conductivity, W/K; T_{sat} is bubble point of LNG, K; h_{tb} is transition boiling heat transfer flux, W/m²; \bar{d}_l is mean characteristic length of LNG, m; Q_{eb} is explosive boiling transfer heat, W; K_c is condensation coefficient; K_e is evaporation coefficient; m_{IV} is mass transfer coefficient, kg/s.

Table 3-1 Substances Parameters for $T_{\text{leidenfrost}}$, T_C , and T_{SLT}

T Substances	$T_{\text{leidenfrost}}$ (K)	T_C (K)	T_{SLT} (K)
Methane	161	191	168
Ethane	249	305	269
Propane	312	370	326

(4) NG vapor dispersion

The model of Box consists of empirical correlations between a set of independent variables that determine the gross properties of the dense gas dispersion process. The correlation is given by

$$\frac{dr_c}{dt} = 1.414 \sqrt{gh_c(t) \left(\frac{\rho_c(t) - \rho_a}{\rho_a} \right)} \quad (3.14)$$

As $(\rho_c - \rho_a)/\rho_a < 0.01$, the dense gas dispersion process is end, and passive diffusion occurs. Situations where the dispersion of a puff or cloud of material is governed solely by the atmospheric turbulence are called passive diffusion. The Gaussian distribution is mostly used, and given by

$$C_{(x,y,z,t)} = C_t \int_{-R_t}^{R_t} \frac{\exp\left[-\frac{(x-x_s-u_0t)^2}{2\sigma_x^2(x-x_0-x_s)}\right]}{\sqrt{2\pi}\sigma_x(x-x_0-x_s)} dx_s \int_{-\sqrt{R_t^2-x_s^2}}^{\sqrt{R_t^2-x_s^2}} \frac{\exp\left[-\frac{(y-y_s)^2}{2\sigma_y^2(x-x_0-x_s)}\right]}{\sqrt{2\pi}\sigma_y(x-x_0-x_s)} dy_s \int_0^{H_t} \frac{\exp\left[-\frac{(z-z_s)^2}{2\sigma_z^2(x-x_0-x_s)}\right] + \exp\left[-\frac{(z+z_s)^2}{2\sigma_z^2(x-x_0-x_s)}\right]}{\sqrt{2\pi}\sigma_z(x-x_0-x_s)} dz_s \quad (3.15)$$

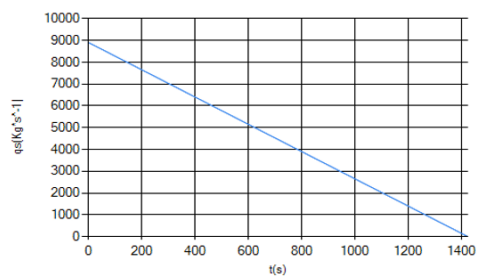
Where r_c is dense gas cloud radius, m; h_c is dense gas cloud height, m; ρ_c is dense gas cloud density, kg/m³; C is Gaussian plume concentration.

3.2 Numerical results of releasing on water

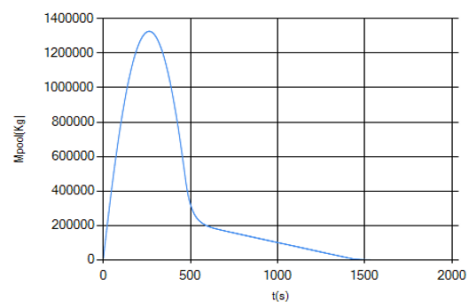
It assumes that LNG is releasing from a fraction hole, and its size is 1.52 m, the hole is 13.98 m below the LNG surface and 0 m/ 3 m/ 5 m on water surface. The LNG carrier tank capacity is 32,658 m³, cross-section area of releasing tank is 949 m², and the rate of loading is 85%~95%. LNG density is 478 kg/m³. NG density is 1.92 kg/m³ at 112 K. LNG component includes CH₄ (95%), C₂H₆ (4%), and C₃H₈ (1%). The C# programming language is used to simulate the process of LNG releasing underwater. By using the numerical models built in the former study, the results are shown in the Table 3.

Table 3-2 Calculation results of releasing on water

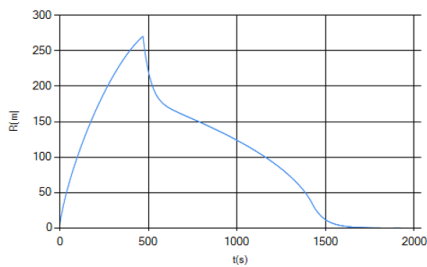
Results Treatment	S ($t=0$) (kg/s)	t_{pool} (s)	r_{max} (m)	r_c (m)	h_c (m)	x_{LFL} ($z=0$, LFL=3.7%)	Initial occurring time of explosive boiling
Without Explosive Boiling ($z_h=0m$)	8901	2037	270	80.2	8.48	700.42	NA
Without Explosive Boiling ($z_h=+3m$)	7889	1401	252	74.5	8.08	744.11	NA
With Explosive Boiling ($z_h=+3m$)	7889	1263	252	74.5	8.08	784.11	486
Errors (%)	0	9.85	0	0	0	-5.37	NA
Without Explosive Boiling ($z_h=+5m$)	7135	1262	237	70.5	7.78	707.71	NA
With Explosive Boiling ($z_h=+5m$)	7135	1142	237	70.5	7.78	744.71	468
Errors (%)	0	9.51	0	0	0	-5.23	NA



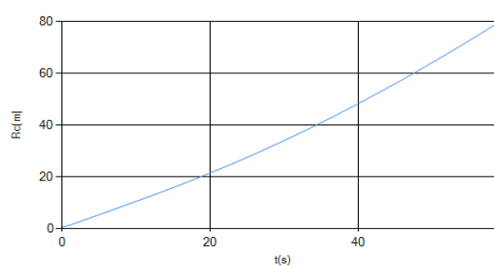
a.



b.



c.



d.

Figure 3-1 Releasing on water 0 m without Explosive Boiling (a. Releasing rate; b. Liquid Pool Mass; c. Liquid Pool Radius; d. Dense Gas Radius)

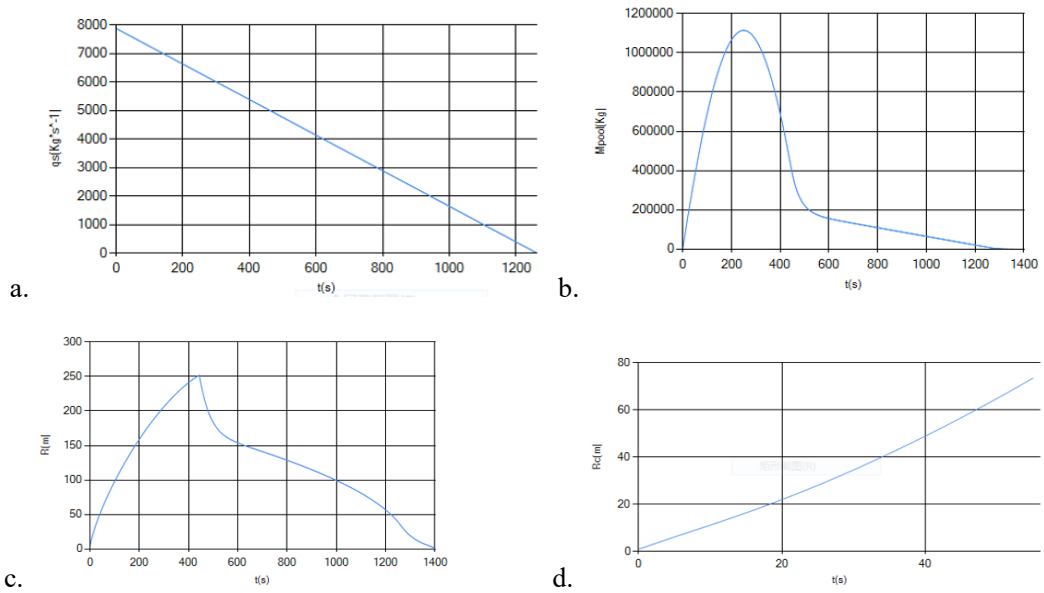


Figure 3-2 Releasing on water 3 m without Explosive Boiling (a. Releasing rate; b. Liquid Pool Mass; c. Liquid Pool Radius; d. Dense Gas Radius)

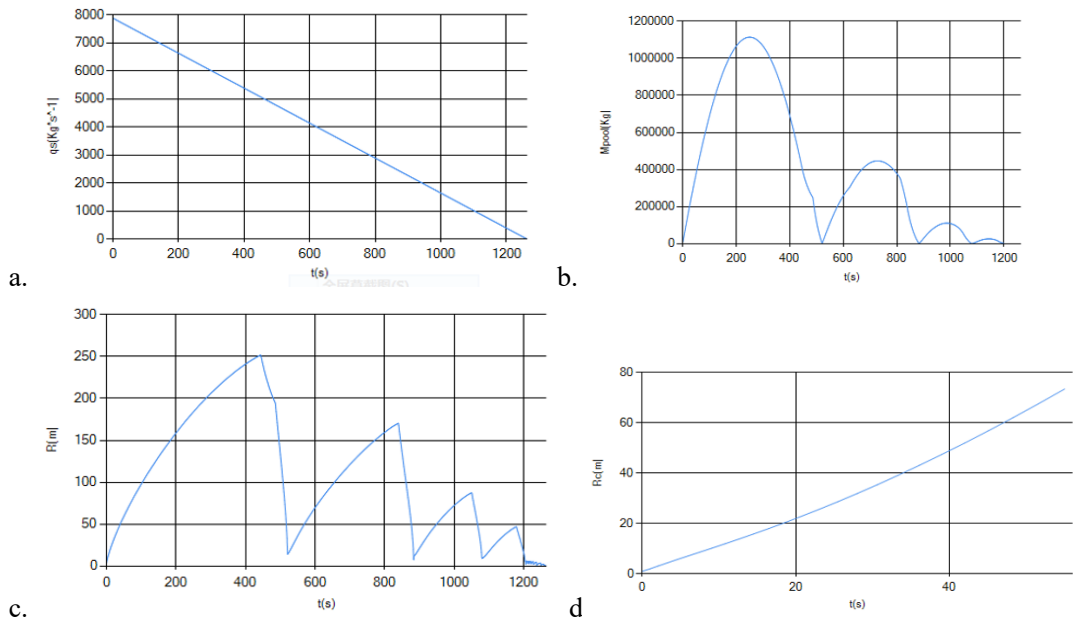


Figure 3-3 Releasing on water 3 m with Explosive Boiling (a. Releasing rate; b. Liquid Pool Mass; c. Liquid Pool Radius; d. Dense Gas Radius)

By comparing Figure 3-1, Figure 3-2 and Figure 3-3, it can be seen that without

considering the influence of explosion boiling, the spreading of LNG on the water surface is in a continuous state, and no pressure shock wave can be predicted. In the case of explosion boiling, with the spreading of the LNG pool on the surface, four times explosion boiling occurs intermittently, with the first one being the most intense. It can be considered that in the process of accident treatment, not only to prevent low temperature frostbite, flammable gas diffusion, but also to prevent the occurrence of uninterrupted explosion boiling. When explosion boiling occurs, the LNG pool will evaporate rapidly, and crew and ship will be surrounded by NG gas cloud with lower temperature, and there will be strong shock wave generation, causing secondary damage to crew and ships around it. In view of this, the selection of appropriate methods to limit the occurrence of explosion boiling is not only conducive to the rapid dispersion of NG gas in the atmosphere, but also can reduce the threat of secondary disasters.

By comparing the data in Table 3-2, it can be found that the occurrence of explosion boiling has no effect on the maximum liquid pool expansion radius, because the maximum liquid pool expansion radius occurs before it. However, it has a great influence on the duration time of liquid pool and the dispersion range of NG. The duration time of the LNG pool will shorten by nearly 10% with the occurrence of explosion boiling, and the diffusion range of combustible gas will expand by 5%. This is because during boiling, the heat flux between LNG and water is nearly 10 times of the maximum heat flux of conventional boiling, which evaporates the LNG in a relatively short time and produces a large amount of cold NG, which shortens the existence time of the pool and expands the range of flammable gas.

By comparing the results of different releasing locations, it can be found that with the increase of the height from the leakage hole to the water surface, the explosion boiling

occurring time will be advanced. But the overall leakage amount will decrease. So the amount of LNG participating in the explosion boiling cannot be simply determined.

3.3 Numerical results of releasing under water

It assumes that LNG is releasing from a fraction hole, and its size is 1.52 m, the hole is 13.98 m below the LNG surface and 0 m/ 3 m/ 5 m under water surface. The LNG carrier tank capacity is 32,658 m³, cross-section area of releasing tank is 949 m², and the rate of loading is 85%~95%. LNG density is 478 kg/m³. NG density is 1.92 kg/m³ at 112 K. LNG component includes CH₄ (95%), C₂H₆ (4%), and C₃H₈ (1%). The C# programming language is used to simulate the process of LNG releasing underwater. By using the numerical models built in the former study, the results are shown in the Table 3-3.

Table 3-3. Calculation results of releasing under water

Results Treatment	S ($t=0$) (kg/s)	t_{pool} (s)	r_{max} (m)	r_c (m)	h_c (m)	x_{LFL} ($z=0$, LFL=3.7%)	Initial occurring time of explosive boiling
Without Explosive Boiling ($z_h=0m$)	8901	2037	270	80.2	8.48	700.42	NA
Without Explosive Boiling ($z_h=-3m$)	7789	1388	250	74.0	8.05	738.1	NA
With Explosive Boiling ($z_h=-3m$)	7789	1247	250	74.0	8.05	779.1	484
Errors (%)	0	10.1 6	0	0	0	-5.56	NA

Without Explosive Boiling ($z_h = -5m$)	6949	1235	234	69.3 3	7.71	696.65	NA
With Explosive Boiling ($z_h = -5m$)	6949	1113	234	69.3 3	7.71	734.65	464
Errors (%)	0	9.87	0	0	0	-5.18	NA

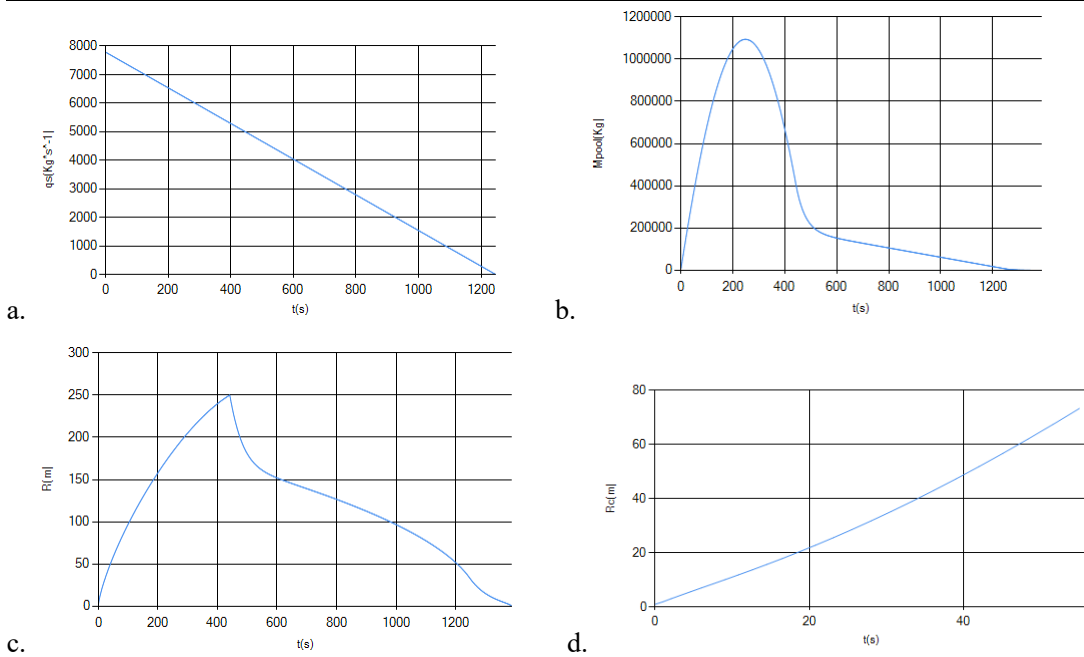
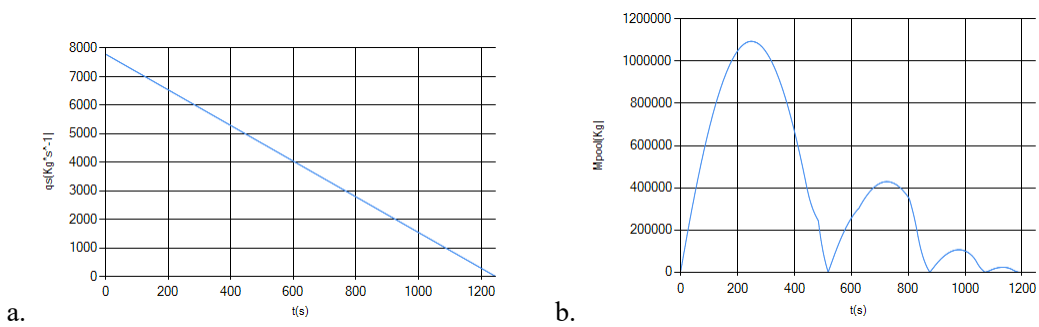
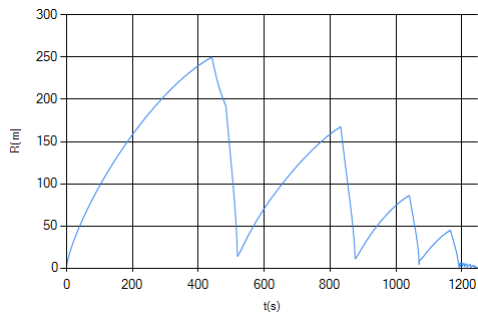
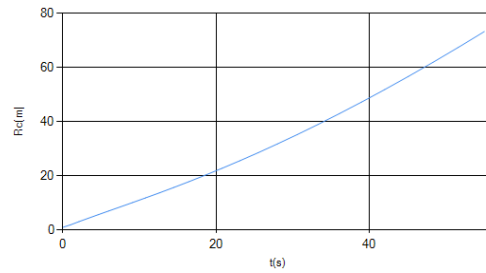


Figure 3-4 Releasing underwater 3 m without Explosive Boiling (a. Releasing rate; b. Liquid Pool Mass; c. Liquid Pool Radius; d. Dense Gas Radius)



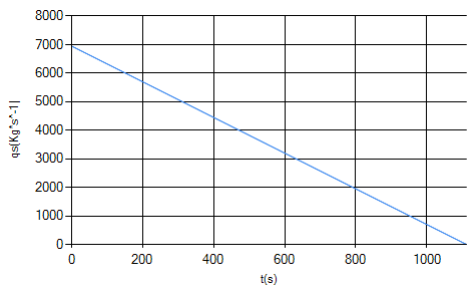


c.

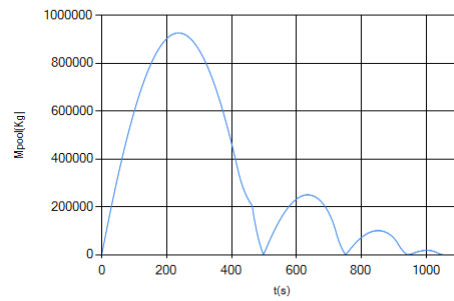


d.

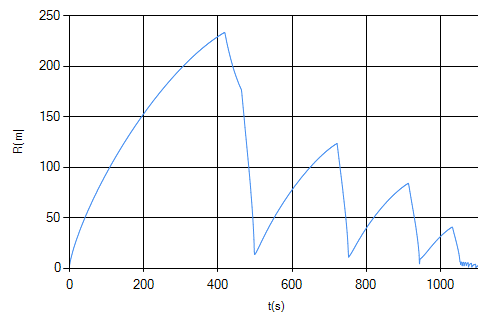
Figure 3-5 Releasing underwater 3 m with Explosive Boiling (a. Releasing rate; b. Liquid Pool Mass; c. Liquid Pool Radius; d. Dense Gas Radius)



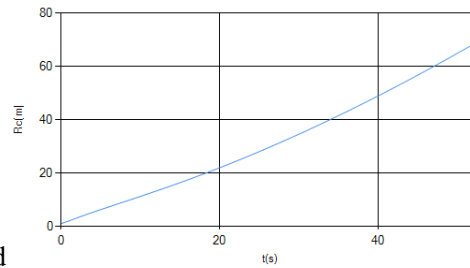
a.



b.



c.



d.

Figure 3-6 Releasing underwater 5 m with Explosive Boiling (a. Releasing rate; b. Liquid Pool Mass; c. Liquid Pool Radius; d. Dense Gas Radius)

From Figure 3-4, Figure 3-5 and Table 3, when LNG releases underwater 3 m, it can be found that the most violent boiling occurs at 484 s after LNG releasing. The pool during time is 10.16% shorter than the without explosive boiling condition. The flammable cloud size is different in the two conditions, explosive boiling makes the size 5.56% bigger than the without explosive boiling condition. Because the NG from explosive boiling is much more than normal boiling during the same time, which

makes air to dissipate the NG in a longer time and the influence area is larger. There are four times of explosive boiling, and the initial one is the most violent one, which has a similar phenomena as releasing on water.

From Figure 3-6, comparing the results of releasing underwater 3 m and 5 m, they have the same trend. The initial mass flow rate, pool duration time and maximum pool radius of releasing underwater 5 m is all smaller than the 3 m condition, but maximum mass and heat transferring rates of the later occurring time is 20s earlier than the former. So we thought that, with the depth of releasing increasing, the initial explosive time will be early. The reason is the heat flux under water is higher than on water, if prolonging the time of underwater process, the methane content in LNG pool formation on water would be lower and the film boiling would more likely finish. Where after, if meeting the decision conditions of explosive boiling mentioned above, it will take place and mass and heat transfer rate will rapidly increase.

Chapter 4 Emergency treatments

Base on the experimental results and numerical results in the last two chapter, there are many conditions taking effect on the LNG releasing accident consequence, e.g. water temperature, releasing position, releasing rate, LNG initial components et al. The traditional emergency treatments can be divided into three methods.

(1) Ejection system

It is an emergency system, which can pump LNG out of storage tank and eject it far away from LNG carrier. When there is an uncontrollable releasing, it can be taken into operation. But there are some issues need your attention. Firstly, the orientation of ejection should be down-wind direction. It should be accompanied by spraying water mist, as a result, the dense gas dispersion time and range can be reduced. Secondly, pay attention to the bubble generation from water, if the bubbles generation rate suddenly decreases, it implies the pressure inside and outside of releasing hole is approached equilibrium which is beneficial for the hole to form ice and block off. At that time, the ejection system should be stopped to prevent building up pressure difference again.

(2) Water mist spraying

It is a conventional firefighting method. But in LNG releasing process, it can make influence on promoting NG dispersion to high altitude of air. When water mist mixes into vapor cloud, it can provide more heat than air to vapor, and as a result, the temperature of NG will be quickly increased and its density will be rapidly reduced.

But it should bear in mind that the water mist should not be directly sprayed onto LNG pool, which can enhance the heat transfer flux and more LNG will boil in a short time that will increase the during time and dispersion scope of dense gas.

(3) Foam spraying on the LNG pool surface

It is a method to limit LNG pool spreading. Because foam can provide more heat flux than air to LNG pool, which can reduce the pool spreading time and scope. At the same time, there is more NG boiling from pool in a short time, which will prolong NG dense gas dispersion time. The NG passes through the foam and absorbs heat from it, as a result, its temperature is increased and density is decreased, which is beneficial for NG to change dense gas dispersion to passive diffusion in a short time.

(4) Limiting the depth of LNG injection into water

Furthermore, if LNG is released on water, there is another important method to reduce hazards. That is to limit depth of LNG injection into water. Because if the water can be seen as infinite heat source, it can provide enough heat to LNG to undergo any boiling style e.g. film boiling, transition boiling, nucleate boiling and explosive boiling. As above analysis, the explosive boiling is a hyperactive boiling phenomenon, which is characterized by transient high heat flux and generation low temperature vapor. From dynamic instability theory, limiting depth of LNG injection into water can reduce explosive boiling occurring opportunity.

The effectiveness of the fourth method (limiting the depth of LNG injection into water) has been verified in the Section 2.3.3 by experiments. Because the experimental research is too dangerous to do, this chapter used the numerical models which are built

up in the Chapter 3 to verify the effectiveness of other methods.

4.1 Initial conditions

It assumes that LNG is releasing from a fraction hole, and its size is 1.52 m, the hole is 13.98 m below the LNG surface. The hole is relatively on and under the water surface. The LNG carrier tank capacity is 32,658 m³, cross-section area of releasing tank is 949 m², and the rate of loading is 85%~95%. LNG density is 478 kg/m³. NG density is 1.92 kg/m³ at 112 K. LNG component includes CH₄ (95%), C₂H₆ (4%), and C₃H₈ (1%). The ejection system transferring rates $m_{ejection}$ set as 500 kg/s and 200 kg/s. The heat flux of foam h_{foam} set as 2000 W/m²·K and 200 W/m²·K. The water mist spraying rate m_{spray} set as 20 kg/s and 10 kg/s. The C# programming language is used to simulate the process of LNG releasing process.

4.2 Results analysis

The results of releasing on and under the water are relatively shown in the Table 4-1 and Table 4-2.

Table 4-1 Results of emergency treating on releasing on the water surface

Results Treatments	$t_{releasing}$ (s)	\overline{m}_{lv} (kg/s)	r_{max} (m)	t_{pool} (s)	r_c (m)	h_c (m)	x_{LFL} ($z=0, LFL=3.7\%$)
No Treatment	1424.0	3116.0	270.0	2037.0	80.2	8.48	700.42
$m_{ejection}=500$ kg/s	1189.9	3133.5	268.8	1836.7	80.2	8.48	702.39
$m_{ejection}=200$ kg/s	1302.6	3140.9	269.8	1938.9	80.2	8.48	703.42
$h_{foam}=2000$ W/(m²·K)	1424.0	3195.0	261.0	1987.0	86.5	8.91	711.90
$h_{foam}=200$ W/(m²·K)	1424.0	3124.0	269.0	2032.0	80.8	8.52	701.68
$m_{spray}=10$ kg/s	1424.0	3116.0	270.0	2037.0	51.2	6.78	682.29

$m_{spary}=20$ kg/s	1424.0	3116.0	270.0	2037.0	48.2	6.59	678.31
---------------------	--------	--------	-------	--------	------	------	--------

Table 4-2 Results of emergency treating on releasing underwater 5m

Results Treatments	$t_{releasing}$ (s)	\overline{m}_{lv} (kg/s)	r_{max} (m)	t_{pool} (s)	r_c (m)	h_c (m)	x_{LFL} ($z=0, LFL=3.7\%$)
No Treatment	1112.2	3133.7	233.8	1235.4	69.33	7.71	696.65
$m_{ejection}=500$ kg/s	896.1	3250.8	231.6	1053.1	69.29	7.70	709.58
$m_{ejection}=200$ kg/s	997.8	3208.7	232.9	1144.4	69.31	7.70	704.62
$h_{foam}=2000$ W/(m ² ·K)	1112.2	3164.4	226.3	1223.5	74.91	8.11	702.81
$h_{foam}=200$ W/(m ² ·K)	1112.2	3137.0	233.0	1234.1	69.89	7.75	697.78
$m_{spary}=10$ kg/s	1112.2	3133.7	233.8	1235.4	48.92	6.51	683.83
$m_{spary}=20$ kg/s	1112.2	3133.7	233.8	1235.4	48.80	6.55	681.59

From Table 4-1 and Table 4-2, there are three main conclusions about emergence treatments effectiveness.

(1) Ejection system plays a major role on reducing releasing time $t_{releasing}$ and liquid pool existing time t_{pool} . But it takes a relatively weak effect on the dense gas diffusion process and maximum pool spreading radius. Because the releasing hole is big enough that the releasing rate is much higher than the ejection rate and the occurring time of dense gas diffusion and maximum pool spreading radius r_{max} is at the early stage of releasing. Furthermore, the mean mass transfer coefficient \overline{m}_{lv} is slightly increased with the existing time of liquid pool decreasing, the x_{LFL} is slightly increasing. As a result of that, ejection system should be accompanied by some other methods to reduce x_{LFL} .

(2) The heat flux of foam plays a major role on reducing LNG pool spreading radius. But it takes a negative effect on the dense gas diffusion process and x_{LFL} . Foam can provide more heat flux than air to LNG and NG, but the NG specific heat capacity is

considerable smaller than LNG. As a result, on the effect of foam heating, there are so much low temperature NG generation in a short time that will increase the dense gas dispersion time and range. This emergency method should also be accompanied by some other methods to increase the NG temperature.

(3) Spraying water mist into NG cloud is considered as the most effective means to reduce dense gas range and x_{LFL} . Because water mist can provide additional heat to NG cloud to increase NG cloud temperature and decrease NG cloud density. But it takes no effect on other factors, such as $t_{releasing}$, t_{pool} , \overline{m}_{lv} , and r_{max} .

4.3 The emergency response on LNG releasing on water

(1) Use foam to cover the surface of the liquid pool. The rapid expansion of the foam prevents the rapid diffusion of the LNG combustible steam and reduces the amount of radiation when the steam catches fire with the ignition source. The expansion rate of the foam is about 500:1. The foam covering on the surface of the LNG liquid tank will increase the evaporation rate of the LNG, reduce the spreading area of the liquid pool, shorten the duration time of the liquid pool, and increase the dispersion range of the NG due to the increase of heat. However, after the NG passing through the foam, the temperature of NG rises, which has a positive effect on reducing the area of NG dispersion. So the use of foam to control NG dispersion can not be simply judged. It is recommended that when using foam covering liquid pool, it is best to combine with spraying water mist, so that NG can be heated in a short time and diffuse into the atmosphere. Spray water mist can not be directed to the liquid pool or leakage port, because it will increase the evaporation rate, which is not conducive to the diffusion of NG by the atmosphere.

(2) Limit the depth of LNG injection into water. When LNG releases on water, floating plates are placed to limit the depth into the water, thereby limiting the possibility of explosion boiling. However, the floating board will slow down the boiling rate. When using this method, it is necessary to combined using water mist or foam to cover the surface of the liquid pool to reduce the duration time and dispersion range of heavy gas cloud. The design of the floating plate is shown in the Figure 4-1.

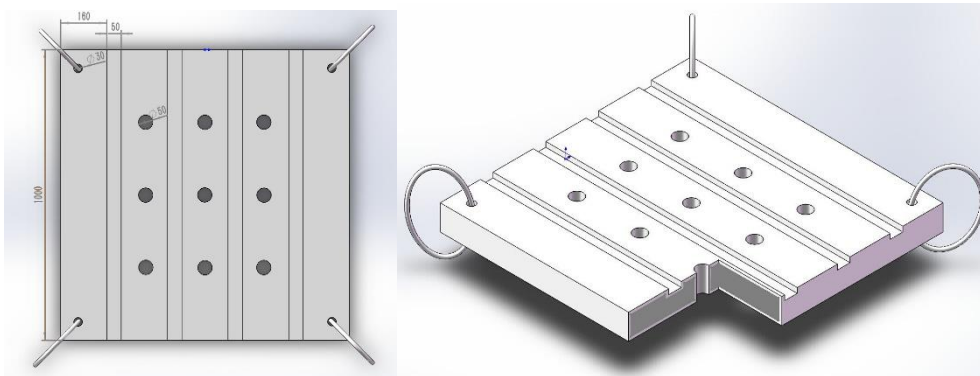


Figure 4-1 Floating plant design

The surface of the floating board is a square with grooves and perforations, the size is 1000 mm×1000 mm×100 mm, and the middle is sandwiched with a high density foam board (high density foam board is a kind of light and high strength board, the thermal conductivity is less than or equal to 0.028 W/(m·K), and the compressive strength can be as high as 350 kPa or more under the condition of the density is not more than 40 kg/m³). The surface with a film of stainless steel (thickness of not more than 2 mm). This design, on the one hand, can ensure that the floating plate floats on the water surface and prevent the LNG spatter sprayed on the floating plate, on the other hand, it has certain strength and low temperature resistance characteristics. The perforation on the float plate is mainly to make part of the water contact with the LNG through the perforations, increase the heat transfer, and shorten the time and range of the existence

of heavy gas on the basis of ensuring that the explosion boiling does not occur. In addition, the four corners of the floating plate are connected with buckles, which is convenient for connection with other floating plates. The number of connecting floating plates can be selected according to releasing rate.

(3) When the carrier is not full load and the stability can meet the requirements, the LNG in the broken tank can be transferring to other tanks which can provide additional capacity.

(4) On the open water, when ship's stability and the surrounding environment condition meet the requirements, start Ejection System, spray out the cargo from the damaged tank to the downwind area away from the ship. This method can reduce the impact of shock wave pressure caused by LNG leakage around the ship and the resulting vapor cloud surrounding the ship or its surrounding offshore facilities.

(5) The emergency workers should select the boarding position away from the leakage location and in the upwind direction. The boarding time should avoid the moment when a large number of steam clouds surrounding the ship. Because at this time, explosion boiling may be occurring or about to occur, so as to avoid the impact of explosion shock wave.

(6) In the rescue process, the emergency workers should always alert to the sudden increase of NG gas, to avoid exposure to visible clouds. As can be seen from the numerical simulation analysis above, several intermittent explosion boiling phenomena may occur in the process of LNG continuous leakage. When there is danger, the emergency team should evacuate the scene in time, or evacuate to the wind direction away from the source of leakage.

4.4 The emergency response on LNG releasing under water

(1) Use foam to cover the surface of the liquid pool. The rapid expansion of the foam prevents the rapid diffusion of the LNG combustible steam and reduces the amount of radiation when the steam catches fire with the ignition source. The expansion rate of the foam is about 500:1. The foam covering on the surface of the LNG liquid tank will increase the evaporation rate of the LNG, reduce the spreading area of the liquid pool, shorten the duration time of the liquid pool, and increase the dispersion range of the NG due to the increase of heat. However, after the NG passing through the foam, the temperature of NG rises, which has a positive effect on reducing the area of NG dispersion. So the use of foam to control NG dispersion can not be simply judged. It is recommended that when using foam covering liquid pool, it is best to combine with spraying water mist, so that NG can be heated in a short time and diffuse into the atmosphere. Spray water mist can not be directed to the liquid pool or leakage port, because it will increase the evaporation rate, which is not conducive to the diffusion of NG by the atmosphere.

(2) The explosion boiling would occur in the process of leakage underwater. The shock wave can break the freezing seal on the LNG vessel, or the partially sealed leak can be reopened. So the emergency treatment for leakage underwater, emergency worker should pay more attention on the NG gas formation. When they found NG sudden increasing, they should be timely evacuation site or evacuated to stay away from the leakage source of wind direction, avoid the damage of blast wave.

(3) When the carrier is not full load and the stability can meet the requirements, the LNG in the broken tank can be transferring to other tanks which can provide additional

capacity.

(4) On the open water, when ship's stability and the surrounding environment condition meet the requirements, start Ejection System, spray out the cargo from the damaged tank to the downwind area away from the ship. This method can reduce the impact of shock wave pressure caused by LNG leakage around the ship and the resulting vapor cloud surrounding the ship or its surrounding offshore facilities.

(5) The emergency workers should select the boarding position away from the leakage location and in the upwind direction. The boarding time should avoid the moment when a large number of steam clouds surrounding the ship. Because at this time, explosion boiling may be occurring or about to occur, so as to avoid the impact of explosion shock wave.

Chapter 5 Conclusion and Suggestions

5.1 Conclusion

5.1.1 Experimental research summary

(1) There are four main instability theories used in analyzing cryogen injection into water process. If the relative velocity between cryogen and surrounding fluid is high enough, the breaking of liquid column or droplets will be defined by the Kelvin-Helmholtz instability and Weber number theory. Furthermore, strong Marangoni effect on vapor film breaking can be obviously observed at the beginning of column floating upwards or the ending of column going downwards. And the periphery of the vapor film near the head of column is considerably stronger than other regions in the effect of Marangoni convection.

(2) When LNG is injected into unconfined water in the pressure of 7 bar, the explosive boiling remarkably occurs with high heat transfer performance. The maximum heat transferring flux can be over 1.9 MW/m^2 . It is ~ 7.8 times bigger than the theoretical limit of heat transferring flux of the pure liquefied methane nucleate boiling (0.244 MW/m^2).

(3) Besides water temperature, both injection pressure and depth of injection into water influence explosive boiling occurring and its heat transfer performance.

(4) According to the images of bubble behaviors, LNG and LN_2 injection processes undergo a similar boiling, that is explosive boiling, which is characterized by bubbles

cloud that strengthens heat transferring rate. LC_3H_8 injection into water triggers subcooled flow boiling. There is no significant breaking on the liquid cryogen column and without bubbles cloud.

5.1.2 Numerical research summary

(1) In the case of explosion boiling, with the spreading of the LNG pool on the surface, several times explosion boiling occurs intermittently, with the first one being the most intense. It can be considered that in the process of accident treatment, not only to prevent low temperature frostbite, flammable gas diffusion, but also to prevent the occurrence of uninterrupted explosion boiling.

(2) The occurrence of explosion boiling has no effect on the maximum liquid pool expansion radius, because the maximum liquid pool expansion radius occurs before it. However, it has a great influence on the duration time of liquid pool and the dispersion range of NG. The duration time of the LNG pool will shorten by nearly 10% with the occurrence of explosion boiling, and the diffusion range of combustible gas will expand by 5%.

(3) With the height or depth of releasing location increasing, the initial explosive time will be early. The reason is the heat flux under water is higher than on water, if prolonging the time of on or underwater process, the methane content in LNG pool formation on water would be lower and the film boiling would more likely finish. Where after, if meeting the decision conditions of explosive boiling, it will take place and mass and heat transfer rate will rapidly increase.

5.1.3 Emergency treatments summary

(1) Ejection system plays a major role on reducing releasing time $t_{\text{releasing}}$ and liquid pool existing time t_{pool} . But it takes a relatively weak effect on the dense gas diffusion process and maximum pool spreading radius.

(2) The heat flux of foam plays a major role on reducing LNG pool spreading radius. But it takes a negative effect on the dense gas diffusion process and x_{LFL} . Foam can provide more heat flux than air to LNG and NG, but the NG specific heat capacity is considerable smaller than LNG.

(3) Spraying water mist into NG cloud is considered as the most effective means to reduce dense gas range and x_{LFL} .

(4) When LNG releases on water, floating plates are designed and placed to limit the depth into the water, thereby limiting the possibility of explosion boiling. However, the floating board will slow down the boiling rate. When using this method, it is necessary to combined using water mist or foam to cover the surface of the liquid pool to reduce the duration time and dispersion range of heavy gas cloud.

5.2 Suggestions

LNG carrier leakage accident is a complicated and changeable process. The variability is not only reflected in the changing environment at the time of leakage, but also in the changing physical process of LNG during the leakage process, among which there are many influencing factors that are difficult to determine. Although this paper

has done a lot of research work on this process, there are still many regrets and deficiencies in the research. Further research work should be mainly focused on the following points:

(1) Due to the high cost and risk of LNG releasing underwater experiment, and the monitoring equipment is not fully able to observe the explosion boiling phenomena, there is a lack of verification of experimental data in the simulation calculation of LNG releasing underwater.

(2) When explosion boiling occurs in LNG releasing underwater process, the influence of thermal fracture cannot be ignored. However, there is no way to make a quantitative mathematical description of the thermal fracture process at present. Meanwhile, the pressure wave generated by explosion boiling cannot be calculated numerically. Therefore, the future research should focus on the numerical models.

(3) The emergency treatment methods proposed in this paper have yet to be tested in practice.

References

- Peibin Diao, Yufan Wang. Natural gas development review and trend analysis in China[J]. China Huaidian Technology Group Company Limited, Beijing, 100070, China, 2019, 41(11):9-11+25.
- Bo Cao. The Global LNG demand stirs the pattern of ship market [J]. Marine Equipment/Materials & Marketing, 2018(06):23-26.
- Wuchao Wu, Tianming Ding, Yijun Fang, Wanzheng Ai. Analysis and prevention of ship Traffic accidents in Zhoushan waters [J] Shipping Management, 2017, 39(05):28-31.
- Minghui Zhang, Xiushuo Chen, Mokai Chou, Lijia Xia, Xijun Guan.. Statistics and analysis of ship traffic accidents in Qingdao [J]. Shipping Management, 2017, 39(10):24-26.
- Jiahui Kang.. Risk analysis and insurance plan research of LNG shipping .[D]. Shenyang: Shenyang University of Aeronautics and Astronautics, 2019.
- D.R.BLACKMORE, M.N.HERMAN, J.L.WOODWARD. Heavy gas dispersion models[J]. Journal of hazardous materials, 1982, 6(1-2).
- J.S.PUTTOCK, D.R.BLACKMORE, G.W.COLENBRANDER. Field experiments on dense gas dispersion[J]. Journal of hazardous materials, 1982, 6(1-2).
- R.P.KOOPMAN, R.T.CEDERWALL, D.L.ERMAK, et al. Analysis of Burro series 40-m³ lng spill experiments[J]. Journal of hazardous materials, 1982, 6(1-2)
- Ruifeng Qi, Phani K. Raj, M. Sam Mannan. Underwater LNG release test findings: Experimental data and model results[J]. Journal of Loss Prevention in the Process Industries, 2011, 24(4).
- D.S. Wen, H.S. Chen, Y .L. Ding, P. Dearman. Liquid nitrogen injection into water: Pressure build-up and heat transfer[J]. Cryogenics, 2006, 46(10).
- H. Clarke, A. Martinez-Herasme, R. Crookes, D.S. Wen. Experimental study of jet structure and pressurisation upon liquid nitrogen injection into water[J].

- International Journal of Multiphase Flow, 2010, 36(11).
- R.C. Duckworth, J.G. Murphy, T.T. Utschig, M.L. Corradini, B.J. Merrill, R.L. Moore. Analysis of Liquid Cryogen-Water Experiments with the Melcor Code[J]. Fusion Technology, 2001, 39(2P2).
- Urith ARCHAKOSITT, Sunchai NILSUWANKOSIT, Tatchai SUMITRA. Effect of Volumetric Ratio and Injection Pressure on Water-Liquid Nitrogen Interaction[J]. Journal of Nuclear Science and Technology, 2004, 41(4).
- Xiaomin Gu, Shuiming Shu. Analysis of Heat Transfer for Cryogenic Liquid Underwater Emission [J]. Energy technology .2006(01):1-3+6.
- Jun Li. Heat Transfer Analysis of the Cryogenic Liquid Drained Directly into Water and Experimental Investigation of the Draining under Near-atmospheric Pressure [D]. Wuhan: Huazhong University of Science and Technology,2004.
- Yi Guo. A Study on Flow and Heat Transfer between Phases for Cryogenic Liquid Drained Directly into Water [D]. Wuhan: Huazhong University of Science and Technology, 2005.
- Bin Zhang, Wanqing Wu, Xingdong Zhang, Yi Zhang, Chuanlin Zhang, Haoran Zhang, Peng Wang. Experimental Study on Ice Forming Process of Cryogenic Liquid Releasing underwater[J]. IOP Conference Series: Earth and Environmental Science, 2017, 94(1).
- Xiaoyang GaoMechanistic Study of the Boiling Mode Changed for the LN2 Discharge under Water [D]. Dalian: Dalian Maritime University,2014
- Porteous W.M., Reid R.C. Light hydrocarbon vapor explosions. Chemical Engineering Progress, 1976, 72 (3):83-89.
- Reid R.C. Rapid phase transitions from liquid to vapor. Advances of Chemical Engineering, 1983, 12 (2):105-208.
- NAIL SULEIMAN KHABEEV. Simulation of vapour explosions[J]. Applied energy, 1999, 64(1-4).
- Dmitrii O.Dunikov, Vasillii V.Zhakhovskii, Stanislav P. Malysenko. Properties of a liquid-gas interface at high-rate phase transitions. Heat Transfer Proceedings of

11th IHTC, 2003, 2:589-599

S.H.Park, J.G. Weng, C.L.Tien. A molecular dynamics study on surface tension of microbubbles. *Int. J. Heat and Mass Transfer*, 2001, 44: 1849-1856.

A.K.M.M. Morshed, Taitan C. Paul, Jamil A. Khan. Effect of nanostructures on evaporation and explosive boiling of thin liquid film: a molecular dynamics study. *Applied Physics A*, 2011, 105:445-451.

Zhaoyi Dong. Experimental and theoretical study on the explosive boiling of saturated liquid nitrogen [D]. Beijing: Graduate School of Chinese Academy of Sciences (Institute of Engineering Thermophysics),2005.

Xingpeng Liu, Li Han, Jinjing Ma Kaihua Guo. Numerical simulation of rapid phase transition caused by LNG spills into water and results interpretation [J]. *Chemical Engineering of Oil and Gas*2016, 45(06):99-104.

Ho Teng, Akihiro Yamasaki. Effect of hydrates on instability of liquid CO₂ jets in the deep ocean, *Energy*, 2003, 22(2-3): 273-278.

Yuraka Abe. Study on thermal-hydraulic behavior during molten material and coolant interaction, *Nuclear Engineering and Design*, 2004, 230:277-291.

Minghao Yuan. Numerical Study on the Mechanisms of the Phenomena Involved in Vapor Explosions [D]. Shanghai: Shanghai Jiaotong University, 2008.

Minghao Yuan, Yanhua Yang, Tianshu Li, Zhihua Hu. Numerical simulation of film boiling on a sphere with a volume of fluid interface tracking method. *Int. J. of heat mass transfer*, 2008, 51(7-8):1646-1657.

Van P. C. (1992) *LIQUID-VAPOR PHASE-CHANGE PHENOMENA:An Introduction to the Thermophysics of Vaporization and Condensation Processes in Heat Transfer Equipment.*: Hemisphere Publishing corporation, USA. pp. 311-318.

Byoung J. K., Jong H. L., Kyung D. K. (2015) Rayleigh-Taylor instability for thin viscous gas films: Application for critical heat flux and minimum film boiling. *International Journal of Heat and Mass Transfer*, 80: 150-158.

Hyun G. L., Junseok K. (2015) Two-dimensional Kelvin-Helmholtz instabilities of

multi-component fluid. *European Journal of MechanicsB/Fluids*, 49: 77-88

Tang J. G., Zhu G. Y., Sun L. C. (2013) Microbubble emission boiling in subcooled pool boiling and the role of Marangoni convection in its formation. *Experimental Thermal and Fluid Science*, 50: 97-106.

LUKETA-HANLIN A. (2006) A review of large-scale LNG spills: experiments and modeling. *Journal of Hazardous Materials*, 132: 119-140.